CHAPTER 6

PROPAGATION EFFECTS ON MOBILE-SATELLITE SYSTEMS

6.1 GROUND WAVES AND EFFECTS OF TERRAIN

Previous chapter have dealt largely with atmospheric effects on radio-wave propagation, the exception being Sec. 5.3 which considers effects of vegetation. Terrestrial telecommunication links and earth-space transmissions, especially at small elevation angles or between satellites and mobile systems, however, may also be influenced by the electrical properties of the Earth's surface and by features of terrain: This section deals with ground waves and obstruction or shadowing by terrain or structures. Section 6.2 treats the physical phenomena of specular reflection and diffuse scatter by the Earth's surface, and Sec. 6.3 relates these phenomena to system design considerations. Sections 6.4, 6.5, and 6.6 give attention to land-mobile, marine-mobile, and aeronautical-mobile systems, and the final Sec. 6.7 describes the Global Positioning System (GPS). All of the major propagation effects on satellite mobile systems (not only the effects of terrain) are given at least brief mention in Sees. 6.4-6.7.

6.1.1. Ground Waves

One means by which radio waves propagate from one location to another is by groud waves. In analyzing propagation near the Earth's surface, what are referred to as ground waves are often separated into s ace waves and surface waves. A space wave consists of the direct wave from transmitter to receiver and the reflected wave, if any, that reaches the receiver after reflection from the Earth's surface. It is the surface wave that is most strongly affected by the electrical properties of the Earth. The attenuation of the surface wave is high and surface wave propagation is limited to short distances for high frequencies. The surface wave is the principal component of the ground wave for frequencies of a few MHz, is of secondary importance at VHF (30-300 MHz), and can be neglected for frequencies greater than 300 MHz (Burlington, 1977).

An approximate expression for the attenuation or loss factor L_s for a surface wave is

$$L_S = \frac{-1}{1 - j2\pi d/\lambda \, (\sin \theta \text{ t } Z)^2} \qquad (6.1)$$

where

$$z = (K - j \sim - \text{COS}^2 6) \text{“} 2 \qquad (6.2)$$

for horizontal polarization and

$$z = \frac{(K - j \frac{\sigma}{\omega \epsilon_0} - \cos^2 \theta)^{1,2}}{\cdot \quad K - j (\sigma / \omega \epsilon_0)} \qquad (6.3)$$

for vertical polarization. Ls has a maximum value of unity. The expression is most accurate for $L_S \leq 0.1$ and within 2 dB in amplitude in any case but is in error in phase by 180 deg as Ls approaches 1 (Burlington, 1 977). In the above expressions $\sigma/\omega\epsilon_0$ can be replaced by its approximate equivalent $60 \sigma\lambda$. The conductivity σ is in mhos/m, θ is the elevation angle, $\omega = 2\pi f$ where f is frequency, ϵ_0 is the electric permittivity of empty space (8.854×10^{-12} F/m), and K is relative dielectric constant. If using $60 \sigma\lambda$, λ is in m. Surface waves are most important at frequencies below the 100 MHz lower limit of this handbook and in a region within a few wavelengths of the ground. They can be neglected in most applications of microwave mobile communications (Jakes, 1974, where the microwave range is treated as from about 450 MHz to 10 or 20 GHz). A more thorough treatment of surface waves can be found in Jordan and Balmain (1968). Ground-wave propagation at frequencies from 10 kHz to 30 MHz is treated in CCIR Recommendation 368-5 (CCIR, 1986a).

6.1.2 Effects of Obstructions

Obstructions along a path in the form of hills and buildings introduce loss with respect to free-space propagation, and the loss varies with time because tropospheric refraction varies with time.

For considering the effect of obstructions, the concept of Fresnel zones is useful. To introduce this topic consider Fig. 6.1 which shows two paths TPR and TSR between a transmitter T and receiver R. TPR is a direct path, and TSR is longer than TPR. If TSR = TPR + $\lambda/2$ where λ is wavelength, the region within the radius r (in the plane perpendicular to TR), at a distance d_T from T and d_R from R, is defined as the first Fresnel zone. The particular value of r in this case is the first Fresnel zone radius and is designated as F_1. The concept can be extended to the case that TSR = TPR + $n\lambda/2$, for which the corresponding Fresnel zone radius can be designated as F_n. The significance of the first Fresnel zone is that all the elements of radiation passing through this zone have components of electric field intensity that add constructively Radiation passing through the second Fresnel zone (values of r between F_1 and F_2), however, interferes destructively with radiation passing the first Fresnel zone, that passing through the third Fresnel zone adds constructively with that in the first zone but makes a smaller contribution, etc. The princess can be understood in terms of Huygen's principle which states that every elementary area of a wavefront can be regarded as a source of secondary spherical waves. When r is small compared to d_T and d_R, it can be determined that

$$F_1 = \sqrt{\frac{\lambda d_T d_R}{d}} \quad \text{m} \qquad (6.2)$$

where $d = d_T + d_R$ and all lengths are in meters or that

$$F_1 = 17.3 \sqrt{\frac{d_T d_R}{f\, d}} \quad \text{m} \qquad (6.3)$$

if distances are in km, f is measured in GHz, and F_1 is in meters. For the situation that d_T is approximately equal to d the expression for F_1 corresponding to Eq. (6.2) is

$$F_1 = (\lambda d_R)^{1/2} \quad (6.4)$$

The value of F_n is related to that for F_1 by

$$F_n = n^{1/2} F_1 \quad (6.5)$$

One might think that a satisfactory signal amplitude would result on a telecommunications link as long as a direct line of sight from the transmitter to the receiver is provided, but consideration of Huygen's principle suggests that having a direct line of sight may not be sufficient. The analysis of the effect of an obstruction approximating a knife edge is given in texts on optics, for example that by Jenkins and White (1976), and in Jordan and Balmain (1968). The results are conveniently expressed in terms of the ratio h_c/F_1 of path clearance h_c to the first Fresnel zone radius F_1, as in Fig. 6,2. If the edge of the knife-edge obstruction is at the direct line of sight, a loss of 6 dB is encountered. To avoid attenuation a clearance of about 0.6 F_1 is required, Note that Fresnel zone analysis is in terms of field intensity. For zero clearance the total field intensity at the receiver location is reduced to O.5 of the value for a completely unobstructed path, A reduction of field intensity to 0.5 corresponds to a reduction of power to 0.25 and therefore to the loss of 6 dB. In analyses of diffraction a parameter v equal to 21'2 h_c/F_1 may be utilized and resulting values of attenuation may be plotted as a function. of v. The parameter v is used, for example, in CCIR Report 715-2 (CCIR, 1986b) and in Jordan and Balmain (1968).

The field intensity beyond an obstacle is dependent upon the form of the obstacle. The loss due to a knife-edge obstacle at grazing incidence is 6 dB, but the corresponding value for a smooth earth is about 20 dB (Burlington, 1977). Formulas and nomograms for determining the loss due to diffraction by a smooth spherical earth are given in CCIR Report 715-2. This same report discusses propagation over irregular terrain, and Hall (1979) treats this difficult topic. Multiple knife-edge diffraction is the subject of a paper by Deygout (1966). He finds which knife-edge obstacle causes the greatest loss and determines this loss. Then locations and

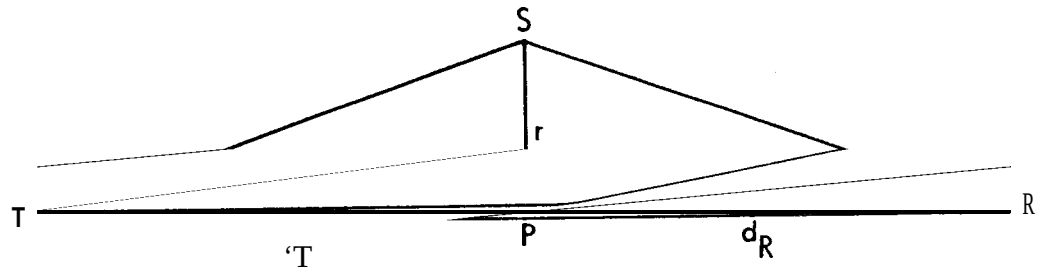

Figure 6.1. Geometry for consideration of Fresnel zones.

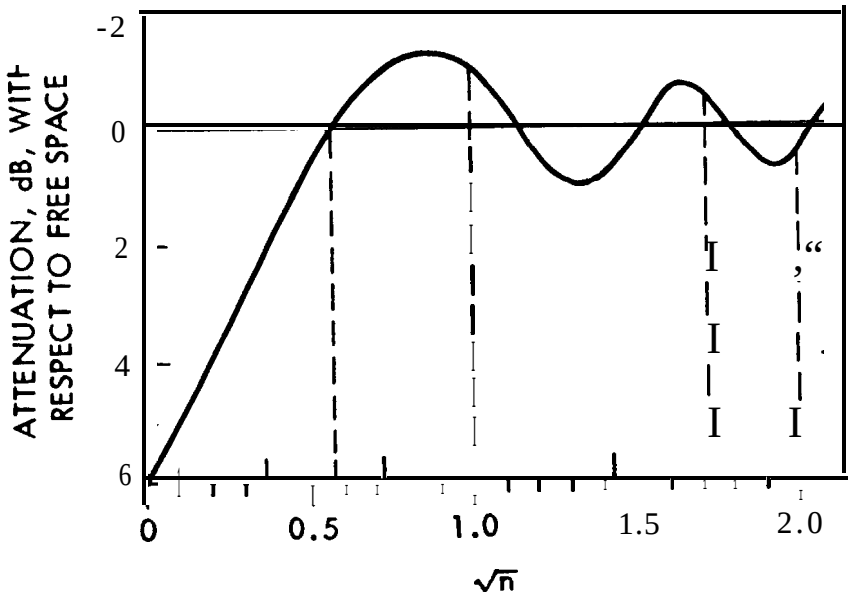

Figure 6.2. Attenuation due to knife-edge diffraction with relation to free space, as a function of $h_c/F_1 = n^{1/2}$ (Hall, 1979).

additional losses are calculated for the other knife-edge obstacles. Assis (1971), noting that the assumption of a knife edge often gives overly optimistic results, employs the approach of Deygout but applies it to the case of rounded obstacles. He provides a set of curves (Fig. 6.3) which give loss asa function of H/F_1, where H is the height of the obstacle above a direct unobstructed path from transmitter to receiver, and a parameter α where

$$\alpha = \lambda^{2/3} r^{1/3}/F_1 \qquad (6.6)$$

with λ the wavelength, r the radius of curvature, and F_1 the first Fresnel zone radius. Note that the condition $H/F_1 = -0.6$ corresponds to $h_e/F_1 = 0.6$ and to free space propagation. Also $H/F = 0$ and $\alpha = 0$ is the condition for the loss of 6 dB mentioned for knife-edge diffraction, and $H/F_1 = 0$ and $\alpha = 1.5$ corresponds roughly to the loss of 20 dB mentioned earlier as well. For positive values of H/F_1, corresponding to obstructions extending above the lowest direct obstructed path, losses are shown to increase above those for H/F_1. An alternative approach to propagation over irregular terrain utilizes an integral equation theory (Ott, 1971) instead of diffraction theory.

It is possible for the signal beyond an obstacle, such as a mountain, to be larger than if the obstacle was not present. This condition occurs due to diffraction alone in the case of a knife-edge obstacle as in Fig. 6.2, where there is a direct line-of-sight path and the obstacle is below the path. We consider now, however, the situation where there is no direct path, This is the case for which the term obstacle gain is normally applied. In this case multipath propagation occurs as in Fig. 6.4, for example, where four paths exist between a transmitter and receiver on the opposite sides of an obstacle. Obstacle gain depends upon the occurrence of favorable phase relations between the signals arriving over the different paths. It can be destroyed by meteorological variations and thus may be subject to fading but can be used to advantage in certain circumstances (Kirby et al., 1955; Hall, 1979). The losses associated with the occurrence of obstacles on mobile communication systems are commonly referred to shadowing losses.

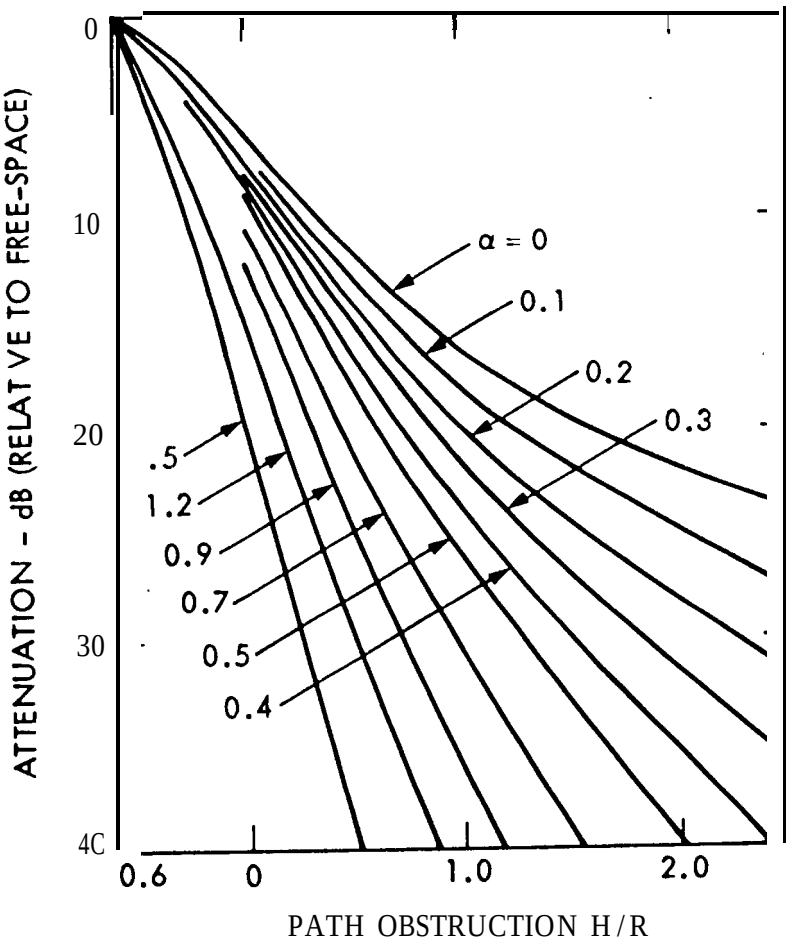

Figure 6.3. Attenuation due to diffraction over obstacles, with relation to free space, as a function of the parameter α and H/R = H/F_1 with H the height of the obstacle above a direct unobstructed path (Assis, 1971).

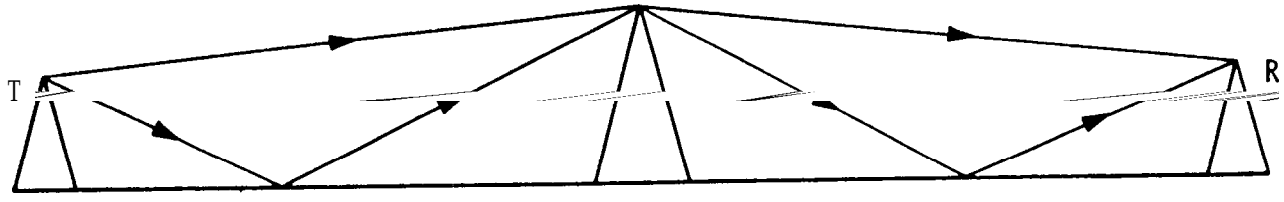

Figure 6.4 Possible ray paths contributing to obstacle gain..

6.2 SPECULAR REFLECTION AND DIFFUSE SCATTER

6.2.1 Introduction

On both earth-space and terrestrial line-of-sight paths, signals may reach a receiving antenna by a direct atmospheric path and by specular reflection and diffuse scatter from the ground. In the following Sec. 6.2.2, expressions are given for total signal amplitude as a function of elevation angle and antenna height for the case of two equal sinusoidal signal components, one traveling overa direct atmospheric path and one experiencing specular reflection from a flat, smooth, perfectly conducting surface. Reflection coefficients for specular reflection from a flat, smooth earth having a finite conductivity are given in Sec. 6.2.3, and surface roughness is taken into account in Sec. 6.2.4. Diffuse scatter is discussed in Sec. 6.2.5, and the factors affecting total signal amplitude are summarized in Sec. 6.2.7.

6.2.2 Multipath Effects

The term multipath refers to a condition in which energy reaches the receiver of a telecommunications system by more than one path. Multipath operation tends to be undesirable, because signals arriving over the different paths tend to arrive with variable relative phase, with the result that they alternately reinforce each other and interfere destructively. The total signal is then characterized by fading involving repeated minima, and the danger exists that the minima will fall below the acceptable signal level. The signals arriving over the different paths also have different time delays which can result in intersymbol interference in digital systems. Multipath ppagation may result from reflection from land and water surfaces and manmade structures. Multipath propagation may also arise from atmospheric effects alone, in the absence of reflection from surface features,

Reflections from a plane surface and the total electric field intensity which results when field intensities arriving over two paths are summed can reconsidered with the aid of Fig. 6.5. The figure shows direct and reflected rays reachig a receiver at a height h_R above a flat, smooth surface at h = 0. The transmitter is

assumed to be so faraway that the two rays can be considered to be parallel at an elevation angle of θ from the horizontal. Assuming also a perfectly conducting surface and horizontal polarization, a 180 deg phase shift will occur upon reflection so that, at h = O, $E_r = -E_i$ where E_r is the field intensity of the reflected wave and E_1 is the field of the incident wave of path 2 of Fig. 6.5. The difference in length of paths 1 and 2, Δl, is $2h_R \sin 6$. If $\Delta l = \lambda/2$ (or $n\lambda/2$ with n odd), maximum total signal intensity will be recorded as the combination of the 180 deg phase shift on reflection and the phase shift of 180 deg corresponding to $\Delta l = \lambda/2$ results in signal reinforcement. If $\Delta l = \lambda$ (or $n\lambda/2$ with n even), destructive

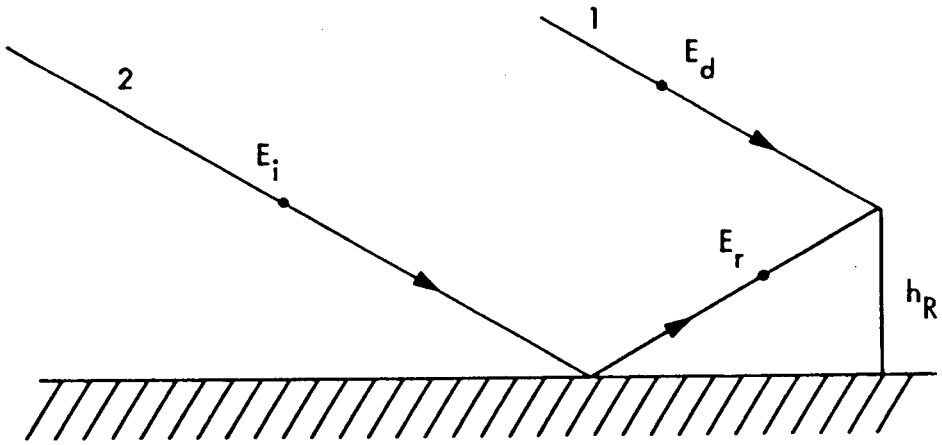

Figure 6.5. Direct and reflected rays for a path employing horizontal polarization (electric-field intensity vectors perpendicular to the plane of the drawing).

interference between the two rays occurs as they then differ in phase by 180 deg. It might seem that satisfactory operation is assured if h_R is chosen so that $\Delta l = n\lambda/2$ with n odd. The discussion to this point, however, has neglected the atmosphere. In the Earth's atmosphere the ray paths will be curved to some degree and variable with time so that constructive and destructive

interference may take place alternately even for a 'fixed receiver location and height. In mobile operations, furthermore, the receiver position with respect to reflecting surfaces will vary and the height will not necessarily be optimum at any particular location.

The phase shift #corresponding to the difference in path length $\Delta l = 2\, h_R \sin\theta$ is given by

$$\phi = (4\pi h_R \sin\theta)/\lambda \qquad (6.7)$$

where λ is wavelength. If the field intensities E_1 and E_2 of rays arriving over the two paths of Fig. 6.5 have the same amplitude E_o, the total field intensity E (Fig, 6.6) is given by

$$|E| = \left| 2\, E_0 \sin \left(\frac{2\pi h_R \sin\theta}{\lambda} \right) \right| = \left| 2\, E_0 \sin \phi/2 \right| \qquad (6.8)$$

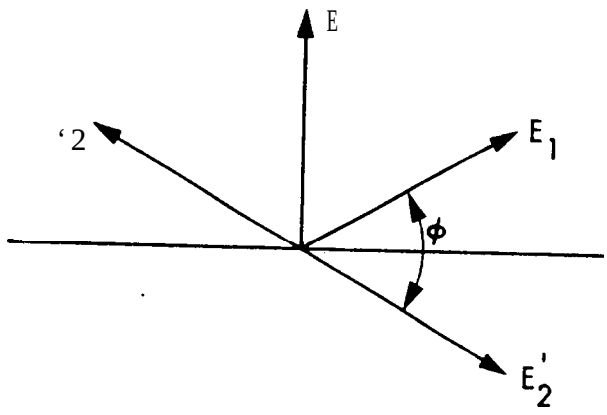

Figure 6.6. Phasor diagram illustrating how field intensities of direct and reflected rays (E_1 and E_2) add to give the total field intensity E.

The two phasors E_1 and E_2 represent field intensities arriving over paths 1 and 2 at the receiver location of Fig. 6.5. In the absence of the phase reversal upon reflection, E_2 would have the direction of E_2'. With phase reversal the vertical components of E_1 and E_2 add to give the result shown, A more general expression for

the amplitude of the total signal when the reflection coefficient may be complex and may not have a magnitude of unity is

$$E = E_o \left[(1 - |\rho|)^2 + 4|\rho| \cos^2(\phi/2) \right]^{1/2} \qquad (6.9)$$

Here $|\rho|$ is the magnitude of the reflection coefficient and ϕ is the sum of the phase of the reflection coefficient and the phase shift corresponding to the path length difference. This expression is given in Beckmann and Spizzichino (1963, p. 224) except that it is shown there with a plus sign in place of the minus sign. Equation (6.9) shows that the maximum and minimum values of E, E_{max} and E_{min} respectively, are given by

$$E_{max} = E_o (1 + |\rho|), \quad E_{min} = E_o (1 - |\rho|) \qquad (6.10)$$

The result is modified further if the transmitting and receiving antennas have gains that are different for the direct and reflected rays. If the transmitter is on a satellite, only the gains of the receiving antenna will be different for the direct and reflected rays. In that case $|\rho|$ should be replaced by the square root of the ratio of the gain for the reflected ray to the gain for the direct ray. Discrimination against the reflected wave by use of antenna directivity is an important potential means for combating multipath effects. This process is more readily accomplished for large elevation angles than for small elevation angles. In modeling low-elevation angle propagation effects for maritime mobile satellite operations, Fang and Ott (1983) assume that the gain of the particular shipboard antenna considered, having a beamwidth of 12 deg, is reduced in the direction of the reflected wave by

$$e^{-(20/7.22)^2}$$

where θ is the elevation angle in degrees. This expression makes use of the fact that the direction of the reflected ray differs from that of the direct ray by twice the elevation angle. Gain is assumed to be power gain here, as is commonly the case, and the square root is taken to obtain the proper ratio for field intensity.

For terrestrial paths, the analysis of how direct and reflected waves combine to reinforce or interfere destructively can be analyzed with the help of Fig. 6.7. For the case that $d >> h_T$ and , $d) > h_R$ and for propagation over a flat earth, $\Delta l = r_2 - r_1 = 2\pi h_T h_R / d$. The corresponding phase difference ϕ is given by

$$\phi = (2\pi/\lambda)(r_2 - r_1) = 4\pi h_T h_R/(\lambda d) \qquad (6.11)$$

For a perfectly conducting surface and assuming equal field intensities E. for the two paths, it develops that, after taking - account of the reversal of phase on reflection,

$$|E| = \left| 2 E_o \sin \left(\frac{2\pi h_T h_R}{\lambda d} \right) \right| = |2 E_o \sin(\phi/2)| \qquad (6.12)$$

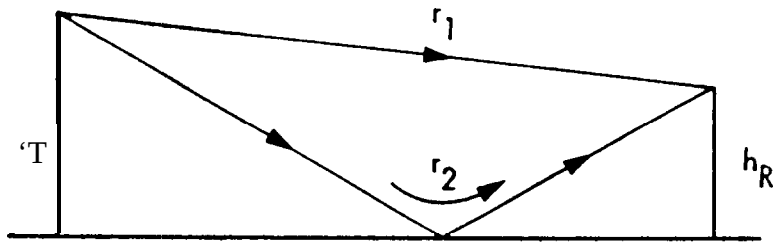

Figure 6.7. Direct and reflected rays for terrestrial path.

The relations for the terrestrial path have been included for comparisen with those for an earth-space path. Equation (6.8) can be obtained from Eq. (6. 12) by replacing h_T/d by $\sin\theta$.

The approaches shown for earth-space 'paths can be modified to take account of earth curvature when necessary (Beckmann and Spizzichino, 1 963; Flock, 1979). Earth curvature affects the phase relation between direct and reflected rays and may also result in a decrease in the magnitude of the reflected ray. The latter condition tends to be most important for aeronautical-mobile systems and is mentioned again in Sec. 6.5.

The different time delays of the signals arriving over the different paths when multipath propagation occurs also tend to be of most importance for aeronautical systems, for which the differences tend to be greatest. The time delays are also of greater importance for digital systems than for analog systems.

The expressions for field intensity E that have been given in this section apply to stable conditions such that, for constant transmitter and receiver heights and locations, signal amplitude is constant. Reflection from flat, smoooth perfectly conducting surfaces is assumed, and the reflection coefficient therefore has a magnitude of unity. The receiving antema is assumed to have the same gain for the reflected ray as for the direct ray, In reality, none of these conditions may be fulfilled. In the following Sec. 6.2.3, expressions are given for reflection coefficients for flat smooth surfaces that have finite conductivity. The magnitudes of the reflection coefficients are less than unity and are different for horizontal and vertical polarization in this case. The antenna gain will very likely be at least somewhat less for the reflected wave than for the direct wave. These modifications help to reduce the effect of the reflected wave but fading due to multipath propagation may still occur. If surface roughness is encountered as well, the magnitude of the reflection coefficient for specular reflection tends to decrease further but diffuse scatter as well as specular reflection must then be taken into account.

6.2.3 Reflection Coefficient for Specular Reflection

The complex electric field intensity E_r of the reflected wave on path 2 at h = O has an amplitude and phase angle that is given by the product of E_i, the electric field intensity of the incident wave at h = O, and the reflection coefficient ρ (Fig. 6.5). Therefore $E_r = \rho E_i$ at h = O and

$$\rho = E_r/E_i \tag{6.13}$$

where all three quantities may be complex. It is evident that the reflection coefficient determines the amplitude and phase of the reflected wave, with respect to the incident wave.

The reflection coefficient for a smooth surface is a function of the relative dielectric constant K, conductivity σ (mhos/m), elevation angle θ, and angular frequency $\omega = 2\pi f$. For a horizontally polarized incident wave the reflection coefficient ρ_h is given by

$$\rho_h = \frac{\sin\theta - \sqrt{K - j\,\sigma/\omega\epsilon_0 - \cos^2\theta}}{\sin\theta + \sqrt{K - j\,\sigma/\omega\epsilon_0 - \cos^2\theta}} \qquad (6.14)$$

The angle θ is measured from the horizontal. The symbol ϵ_0 represents the electric permittivity of empty space, 8.854×10^{-12} F/m.

The expression for ρ_v the reflection coefficient for "vertical" polarization, meaning for the electric field intensity vectors in the plane of incidence (the plane of the drawing as shown in Fig. 6.8), is

$$\rho_v = \frac{[K - j\,\sigma/\omega\epsilon_0]\sin\theta - \sqrt{K - j\,\sigma/\omega\epsilon_0 - \cos^2\theta}}{[K - j\,\sigma/\omega\epsilon_0]\sin\theta + \sqrt{K - j\,\sigma/\omega\epsilon_0 - \cos^2\theta}} \qquad (6.15)$$

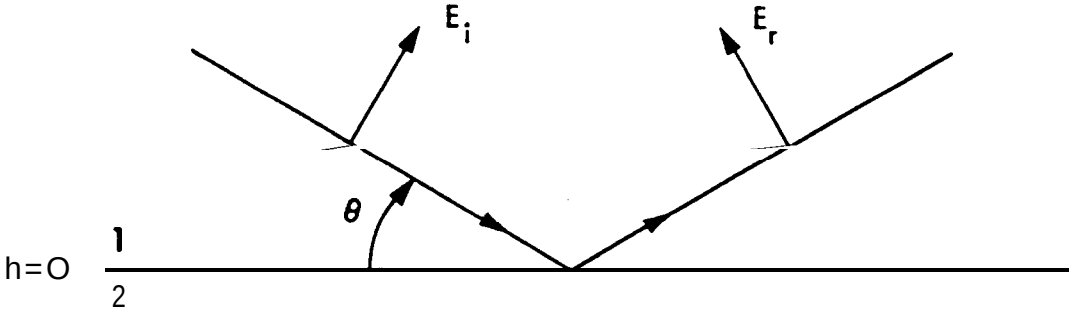

Figure 6.8. Electric field intensity vectors for vertically polarized wave.

Note that the electric field intensity vectors are not strictly vertical unless θ = O deg. The field intensities have horizontal components, and the relation between these horizontal components

at h = 0 is determined by the tangential (horizontal) boundary conditions which apply at this surface. Consistent with Fig. 6.8, it is normally assumed that the vertical components of the field intensities are in the same direction, which means that the horizontal components are automatically taken to be oppositely directed. Thus for a perfectly conducting surface $\rho_v = +1$, consistent with the horizontal components being equal and opposite so that the total tangential field intensity is zero at the surface. Assuming the same perfectly conducting surface and for 6 = 90 deg, where horizontal and "vertical" polarizations are indistinguishable, $\rho_h = -1$. The reason for this discrepancy is the different intial assumptions made about the directions of E_i and E_r for the two polarizations. For horizontal polarization they are assumed to be in the same direction, whereas for vertical polarization the horizontal components are assumed to be in opposite directions as mentioned above. As two vectors pointing in the same direction but 180 deg out of phase are equivalent to two vectors pointing in opposite directions but in phase, the two results are compatible. The reflection coefficient p_v applies to waves having a vertical component of electric field intensity, and the greatest interest usually lies in. the vertical component rather than in the horizontal component. Thus it is appropriate that the sign of ρ_v be chosen to be positive if-the vertical component of E_r is in the same direction as that of E_i. The wave to which ρ_h applies is polarized perpendicular to the plane of incidence. The two types of waves are orthogonally polarized, meaning that their electric field intensity vectors are mutually perpendicular. Both have horizontal components but the horizontal component of the wave polarized in the plane of incidence is perpendicular to the horizontal field intensity of the wave polarized perpendicular to the plane of incidence. Plots of ph and ρ_v are given 'in Fig. 6.9.

An important characteristic of the reflection coeffic ent for vertical Polarization is that in the lossless case p_v goes to zero at the Brewster angle θ_p defined by

$$\theta_p = \tan^{-1} (K_1/K_2)^{1/2} \qquad (6.14)$$

If medium 1 is air so that $K_1 = 1$

$$\theta_p = \tan^{-1} (1/K_2)^{1/2} \qquad (6.15)$$

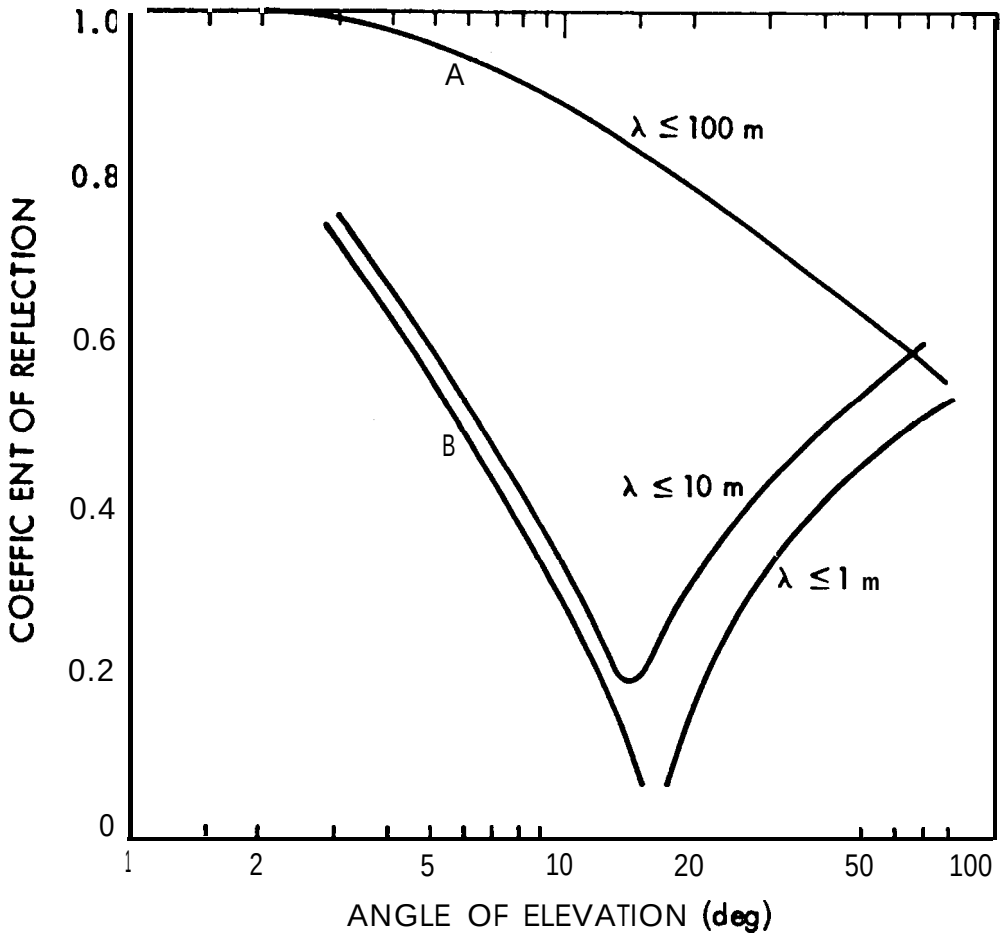

Figure 6.9. Reflection coefficients for plane average ground. A: horizontal polarization; B: vertical polarization (CCIR, 1982). Also see CCIR (1986 c).

For σ not equal to zero, a minimum value of $|\rho_v|$ still tends to occur, and as it is $\sigma/\omega\epsilon_o$ that appears in Eq. (6. 15) the minimum tends to be quite pronounced for large values of ω. See Sec. 6.2.8 for a discussion of the phase of the reflected signal.

Reflection coefficients for circularly polarized waves can be derived from those for horizontal and vertical polarization. When a circularly polarized wave is reflected, the reflected wave contains in general a component of the original circular polarization and a component of the orthogonal or cross polarization. When a right circularly polarized wave is reflected, for example, both right and left circularly polarized waves result. If the elevation angle is less than the Brewster angle [θ_p of Eq. (6. 15)], the original polarization predominates, whereas' if the angle is greater than the Brewster angle the cross polarization predominates. It is shown in Appendix 6.1 that the reflection coefficient for the original polarization ρ_c is given by

$$\rho_c = (\rho_h + \rho_v)/2 \tag{6.18}$$

whereas the coefficient giving the cross polarized component ρ_x can be found from

$$\rho_x = (\rho_h - \rho_v)/2 \tag{6,19}$$

6.2.4 Surface Roughness

The discussion of reflection in Sees. 6.2.1 and 6.2.2 assumed a perfectly smooth reflecting surface, consistent with reflection in the forward direction only. If a surface is rough, however, energy is reflected or scattered in other directions as well, with the result that the magnitude of the forward reflection coefficient is reduced. A commonly accepted criterion for roughness is the Rayleigh criterion, which can be explained with the help of Fig. 6.10. Consider two rays A and B such that ray A follows a path longer that of ray B by π rad, the two rays being reflected from locations that differ in height by Δh. As the two rays differ in phase by π rad they interfere destructively for forward reflection. Therefore some of the incident energy is scattered in other than the forward direction. The amount Δl by which the path length of ray A exceeds that of ray B is given by

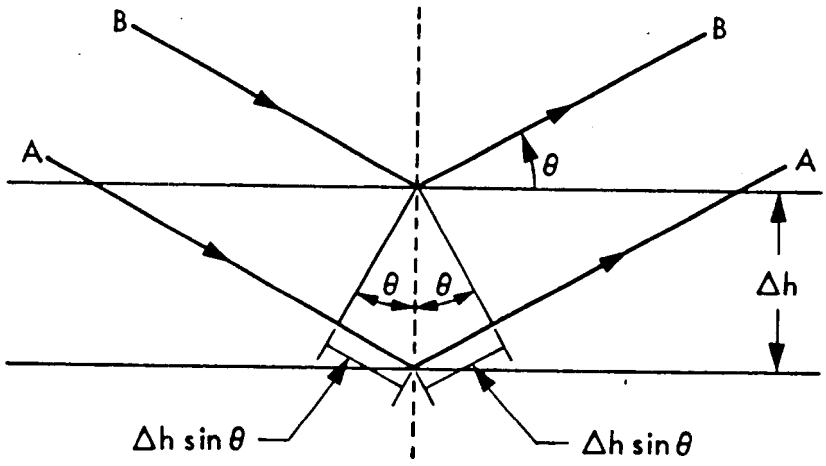

Figure 6.10. Basis for Rayleigh criterion,

$$\Delta\ell = 2\,A\,h\,\sin\theta \tag{6.20}$$

and the corresponding phase difference $\Delta\phi$ equals π so that

$$\Delta\phi = (4\pi/\lambda)\,Ah\,\sin\theta = \pi \tag{6.21}$$

from which

$$\Delta h \geq \frac{\lambda}{4\,\sin\theta} \tag{6.22}$$

has been taken as the criterion for roughness (Beckmann and Spizzichino, 1963). Less well established is a criterion for smoothness, but one form has been

$$\Delta h \leq \frac{\lambda}{8\,\sin\theta} \tag{6.23}$$

except that 8 is arbitrary and it has been recognized that a larger number may be more appropriate.

The specular reflection coefficients ρ_{hs} and ρ_{vs} for reflection from other than a perfectly smooth surface can be related to the coefficients ρ_h and ρ_v, for example by

$$\rho_{hs} = \rho_h\,\rho_s \tag{6.24}$$

and

$$\rho_{vs} = \rho_v \rho_s \qquad (6.25)$$

where ρ_s is surface roughness factor. A form for ρ_s is

$$\rho_s = e^{-(\Delta\phi)^2/2} \qquad (6.26)$$

with

$$\Delta\phi = (4\pi h_s/\lambda) \sin O \qquad (6.27)$$

where h_s is the rms value of the terrain height irregularities, λ is electromagnetic wavelength, and θ is elevation angle. This relation is the same as that used in Eq. (6.21) except that hs is now an rms value and $\Delta\phi$ can take any value. However, Miller, Brown, and Vegh (1984) have asserted that the proper form for ρ_s is

$$\rho_s = e^{-(\Delta\phi)^2/2} I_0[(\Delta\phi)^2/2] \qquad (6.28)$$

where $I_0[(\Delta\phi)^2/2]$ is the modified Bessel function of $[(\Delta\phi)^2/2]$. This Bessel function has a value of unity or greater and its inclusion results in ps being larger than otherwise.

It has been pointed out by E.K. Smith that the criterion for smoothness of Eq. (6.23) when applied to Eq. (6.26) for surface roughness results in values of ps which are not consistent with a smooth surface. For example, if $Ah = \lambda/(8 \sin\theta)$ is used, $\Delta\phi$ becomes $\pi/2$ and the value of ρ_s corresponds to a loss upon reflection of 1 O dB. Such a surface can hardly be considered smooth. If $Ah = \lambda/(24 \sin\theta)$ is used, $\Delta\phi$ becomes $\pi/6$ and the corresponding loss is about 1.2 dB. This value of Ah gives a more reasonable result, but no great importance can be attached to the precise value of 24.

If the relation of Eq. (6.28), which includes the modified Bessel function, is used, the loss upon reflection for $\Delta\phi = \pi/2$ is reduced from 10 dB to 7.7 dB. For $\Delta\phi = \pi/6$, however, 1_0 of Eq. (6.28) is close to unity and the loss is about the same (1.2 dB) as when 1_0 is

omitted. It nevertheless seems desirable to include the modified Bessel function for general use and to take as a criterion for smoothness the relation

$$Ah \leq \lambda/(A \sin \theta) \qquad (6.29)$$

where **A** can be taken as the value of 24 or greater depending upon what loss upon reflection is deemed appropriate.

As large reflection coefficients for forward reflection tend to be undesirable, the occurrence of high degrees of surface roughness of possible reflecting surfaces can generally be looked upon with favor for telecommunication purposes. In the case of reflection from a rough surface some degree of specular reflection may still take place and diffuse scatter occurs as well. Specular reflection is directional, coherent in phase, and tends to have small fluctuations in amplitude. Diffuse scatter exhibits little directivity, is incoherent in phase, and tends to exhibit larger fluctuations which are Rayleigh distributed (Beckmann and Spizzichino, 1963). Section 6.2.6 gives the form of the Rayleigh probability density function.

6.2.5 Diffuse Scatter

With increasing surface roughness. specular reflection decreases in importance and diffuse scatter increases. Using copolarized circular polarization as an example,

$$\rho_{cd} = \rho_d \rho_c \qquad (6,30)$$

where ρ_c is the plane-earth reflection coefficient, ρ_d is a coefficient for diffuse scatter, and ρ_{cd} gives magnitude and phase for the diffusely scattered radiation. The same type of relation is assumed to apply to the other polarizations. The value of ρ_d is commonly taken as 0.35, but Fig. 6.11 shows the theoretical distribution in dB for a combination of specular reflection and diffuse scatter for various values of ρ_d. This combination is described by the Rice probability density function [Eq. (6.43)].

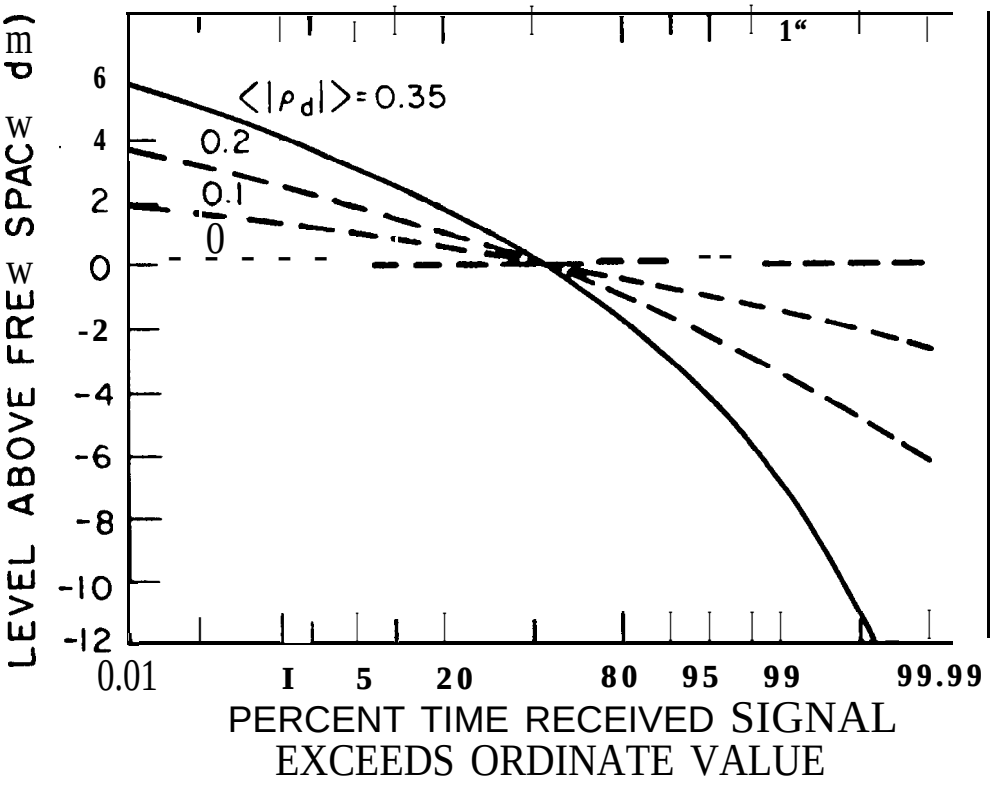

Figure 6.11. Amplitude distributions for signals consisting of specular-reflection and diffuse-scatter components, as a function of diffuse-scatter coefficient ρ_d (Beckmann and Spizzichino, 1963).

6.2.6 Statistical Characteristics of Multipath Signals

In considering the statistics of multipath signals received by moving mobile receivers, a distinction can be made between the rather" rapid fluctuations "that occur over short distances of a few tens of wavelengths when the mean signal is essentially constant and the slower variations that occur as the vehicle moves over large distances and experiences shadowing losses (Jakes, 1974). For analysing the rapid variations, the received field intensity E(t) can be expressed as the sum of two components that are separated in phase by 90 deg such that

$$E(t) = x(t) \cos \omega t + y(t) \sin \omega t \qquad (6.31)$$

The quantities x(t) and y(t) represent the amplitudes of two orthogonal terms, both assumed to have normal or Gaussian distributions with zero mean and the same variance σ^2 such that

$$p(x) = \frac{1}{(2\pi)^{1/2}\,\sigma}\, e^{-x^2/(2\sigma^2)} \tag{6,32}$$

and

$$p(y) = \frac{1}{(2\pi)^{1/2}\,\sigma}\, e^{-y^2/(2\sigma^2)} \tag{6.33}$$

where p(x) and p(y) represent probability densities. Assuming that p(x) are statistically independent, their joint probability density p(x,y) is given by

$$p(x,y) = p(x)\; p(y) = \frac{1}{2\pi\,\sigma^2}\, e^{-(X^2+y^2)/2\sigma^2} \tag{6.34}$$

It is desirable to know the probability density of the total field intensity amplitude which will be designated by r. The relation between r, x', and y is $r^2 = X^2 + y^2$. To determine p(r), one can begin by using the relation (Beckmann, 1967)

$$p(r,\phi) = p(x,y)\; J \tag{6.35}$$

where J is the Jacobian defined by

$$J = \begin{vmatrix} \dfrac{\partial x}{\partial r} & \dfrac{\partial y}{\partial r} \\[2ex] \dfrac{\partial x}{\partial \phi} & \dfrac{\partial y}{\partial \phi} \end{vmatrix} \tag{6.36}$$

The derivatives shown can be evaluated by noting that

$$x = r\cos\phi \tag{6.37}$$

and

$$y = r\sin\phi \tag{6,38}$$

from which

$$J = \begin{vmatrix} \cos\phi & \sin\phi \\ -r\sin\phi & r\cos\#1 \end{vmatrix} = r\,(\cos^2\phi + \sin^2\phi) = r$$

so that

$$p(r,\phi) \qquad \frac{r}{2\pi\sigma^2}\, e^{-r^2/2\sigma^2} \tag{6.39}$$

To obtain p(r) one can integrate with to ϕ from O to 2π with the result that

$$p(r) = \frac{r}{\sigma^2}\, e^{-r^2/2\sigma^2} = \frac{2r}{a}\, e^{-r^2/\alpha} \tag{6.40}$$

where $\alpha = 2\sigma^2$ is the mean square value of p(r). This function is known as the Rayleigh probability density function. The forms of the Rayleigh and norms density functions are shown in Fig. 6.12, where b_o takes the place of σ^2 of Eq. (6.40).

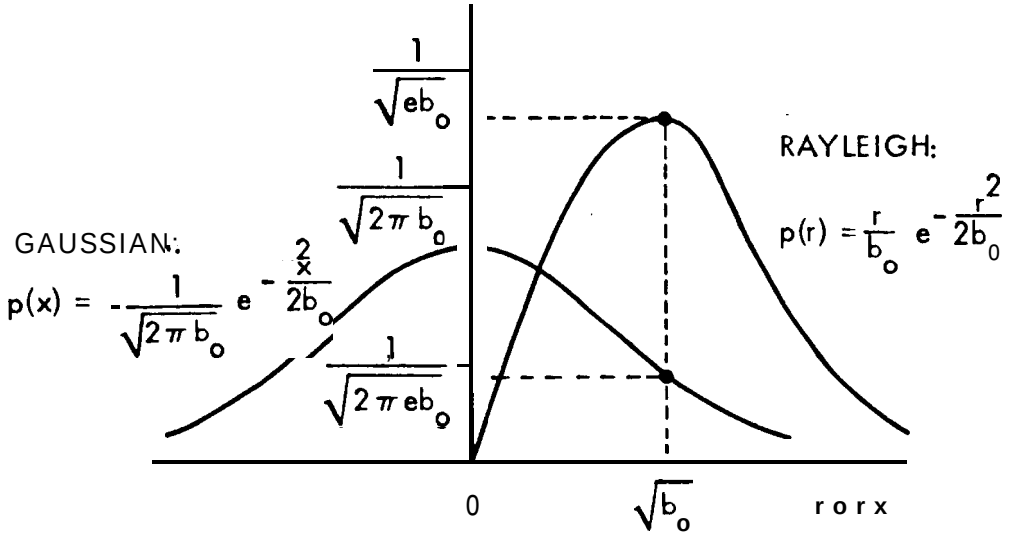

Figure 6.12. Normal and Rayleigh probability density functions (Jakes, 1974).

The probability density for phase in this case $p(\phi)$ is uniform with $p(@) = 1/2\pi$ for $O \leq \phi \leq 2\pi$. Considerable evidence exists to the effect that the signal received by a land mobile receiver in ground-to-ground service is Rayleigh distributed on a local scale. A good approximation to a Rayleigh distribution may occur for as few as four to six multipath components (Schwartz et al., 1966). In some cases when the number of rays is very small, however, the Rayleigh distribution may not apply, The Rayleigh distribution can be considered to be a special case of more general distributions including the m distribution (Panter, 1972) and the Weibull distribution (Beckmann, 1967; Shepard, 1977), and forms of these distributions may be applicable when the Rayleigh distribution is not not.

The logarithmic or decibel forms of the slower deeper variations in mean signal level tend to follow the normal distribution and to have a probability distribution of the form of

$$p(x) = \frac{1}{(2\pi)^{1/2}\sigma} e^{-(x - x_o)^2/2\sigma^2} \qquad (6.41)$$

where $x = \ln y$ with y being the actual field intensity and $x_o = \ln y_o$ with y. the mean field intensity. To obtain the probability density of field intensity y one can-use $p(x)\,dx - = p(y)\,dy$ and note that as $x = \ln y$, $dx = dy/y$ so that $p(y) = p(x)/y$ and

$$P(Y) = \frac{1}{(2\pi)^{1/2}\sigma y} e^{-[\ln (y/y_o)]^2/2\sigma^2} \qquad (6.42)$$

This probability density is known as the lognormal probability density function.

The probability density of the sum of a constant vector and a signal following the Rayleigh distribution, such as the sum of the direct line-of-sight and diffuse scatter components for land-mobile

satellite transmissions, is the Rice or Rice-Nakagami distribution (Norton et al., 1955; Beckmann and Spizzichino, 1963; Beckmann, 1967). The form given by Beckmam for total electric field intensity r is

$$p(r) = \frac{2r}{\alpha} e^{-(r^2 + c^2)} I_0(2cr/\alpha) \qquad (6.43)$$

where c is the field intensity of the constant component, α is the value appearing in the Rayleigh distribution [Eq. (6.40)], and 1_0 is the modified Bessel function of the first kind and zero order. For application to land-mobile operation it is useful to have an expression for signal power written in terms of K, the ratio of power in the steady component to power in the random or diffuse component. A relation given by Davarian (1985) and utilized by Vogel and Smith (1985), etc. is

$$p(s) = (1 + K) e^{[-s(1 + K) - K]} I_0 2[s(1 + K) K]^{1/2} \qquad (6.44)$$

where s is signal power.

Because of its pertinence to satellite or terrestrial land mobile service, attention has been given to combinations of Rayleigh and lognormal fading and Rician and lognormal fading, Rayleigh fading tends to be associated with diffuse scatter, Rician fading with reflection and scatter, and lognormal fading with shadowing by trees, terrain, or structures [Hansen and Meno, 1977; Butterworth, 1985; Loo, 1985; Stutzman, 1985]. Loo (1985) analyzd the sum of Rayleigh and lognormal fading and noted that if the lognormal amplitude is temporarily held constant the resultant probability density is Rician.

6.2.7 Total Signal Amplitude

Factors affecting the total signal amplitude E, arising from the combination of direct and specularly reflected and diffusely scattered waves, can be summarized for linear polarization, using horizontal polarization as an example, by

$$E = E_o \left[1 + g_r(2\theta)\, \rho_s F D e^{j\phi} \rho_h e g_r(\theta_d)\, \rho_{hd}\right] \qquad (6.44)$$

This expression gives no information about the variation of the parameters with time or how the specular and diffuse components combine but does point out the factors that are involved in determining E, which represents total electric field intensity in volts/meter. The quantity g (20) is voltage gain for the specularly reflected wave relative to 'that for the direct wave, with 2 θ indicating that gain refers to an angle that differs by twice the elevation angle θ from that for the direct wave. The factor ρ_s is a roughness factor that is unity or less in magnitude and indicates the degree to which the smooth-earth specular reflection coefficient ρ_h is reduced by surface roughness. F is a factor that can be used to take account of blockage or shadowing by obstacles, including structures, terrain, or vegetation. The theoretical maximum value of F is two, which value would apply if propagation was via only the first Fresnel zone. In practice the value of F is found to be between 0.1 and 1.2 in the majority of cases. D is a divergence factor that takes account of the fact that reflection from a spherical earth tends to result in a decrease in reflected signal intensity as compared to reflection from a flat surface. D is approximately unity for angles θ above about 5 deg. The quantity ϕ represents phase shift due to the difference in path length for the direct and reflected waves, The reflection coefficient phd applies to diffuse scatter, and $g_r(\theta_d)$ stands for voltage gain relative to that for the direct path at an angle θ_d that is an average or effective angle for diffuse scatter Diffuse scatter takes place over a range of angles but θ_d is sometimes taken to be 20 as for specular reflection.

The phase angle # varies with the height of the receiving antenna above the reflectig surface in accordance with Eq. (6.7). For the simple situation whe F = D = 1 and diffuse scatter is negligible, the normalized field intensity will fall within the limits of

$$1 \pm [\, |g_r(2\theta)|\, |\rho_{hs}|\,] \qquad (6.45)$$

where $\rho_{hs} = \rho_h\, \rho_s$ of Eq. (6.44).

For circular polarization similar relations apply but specular reflection in that case results in the production of a cross polarized component as well as a component having the original polarization, as shown by Eqs. (6.18) and (6.19). Antenna gain for the cross polarized component is considerably lower than for the original polarizationat the angle of the direct ray, but antenna gains for the specularly generated components may be comparable for large angles away from the direct ray. The antenna may have different phase responses for the two components. For F = D = 1 and neglecting diffuse scatter, the normalized output voltage of the antenna falls within the limits of

$$1 \pm [\, |g_{cr}(2\theta)|\,|\rho_{cs}| + |g_{xr}(2\theta)|\,|\rho_{xs}| \,] \qquad (6.46)$$

where g_{cr} is the antenna voltage gain for the copolarized reflected wave, g_{xr} is the antenna voltage gain for the crosspolarized wave produced by reflection, p_{Cs} is the rough-surface reflection coefficient for the copolarized wave, and ρ_{xs} is the corresponding coefficient for the crosspolarized wave.

6.2.8 Phase

The phase of the reflected signal, like the amplitude, is a function of relative dielectric constant and conductivity. Values of these parameters for a range of materials, including sea water, fresh water, ice, and ground, are shown as a function of frequency in Recommendation 527-1 (CCIR, 1986d). The phase of the reflection coefficient tends to be close to 180 deg for horizontal polarization for all values of elevation angle. For vertical polarization, the phase tends towards 180 deg for angles less than the Brewster angle [Eqs. (6. 14) and (6. 15) and Fig. 6.9] and O deg for angles greater than the Brewster angle (CCIR, 1986c, Jordan and Balmain, 1968).

6,3 SYSTEM-DESIGN CONSIDERATIONS

6.3.1 Multipath and Fading Measurements

Whereas Sec. 6.2 describes the physical phenomena of specular reflection and diffuse scatter, the present Sec. 6.3 treats related system-design considerations. Data on the effects of reflection and scatter are needed for system design, and Sec. 6.3.1 describes certain measurements that have been carried out in the recent past. Still more recent work conducted to satisfy the needs of land-mobile satellite systems is reported in Sec. 6.4. Section 6.3.2 deals with "the techniques of equalization and diversity for combating multipath effects. Techniques applicable to analog and digital narrow-band systems are described in Sees. 6.3.3 and 6.3.4, respectively, and spread-spectrum systems are introduced in Sec. 6.3.5.

Multipath propagation tends to cause signal fading, and data on fading can be accumulated by making measurements of total signal amplitude under multipath-propagation conditions. In this section, however, the term multipath measurement is used in distinction from fading measurement. Fading is taken to refer to variations of signal amplitude under conditions involving no separation or distinction of the multipath components which contribute to fading. By the term multipath measurement, reference is made here to data taken with high time resolution so as to separate and distinguish the multipath signal components. Both multipath and fading data are useful in planning and analyzing performance of mobile communication systems.

One method of making multipath measurements is to transmit very short plses and to record the signals received over the path of interest. This approach was used by Turin (1980) in a program that involved transmitting 100-ns pulses at carrier frequencies of 488, 1280, and 2920 MHz. Pulses at these three frequencies were transmitted simultaneously at a rate of one per second in urban areas of San Francisco, Oakland, and Berkeley. In such areas, multipath propagation can result from reflections from buildings and other structures as well as from the ground. For a dense, high-rise area, Turin included an illustration showing a signal having a delay of about 3 μs beyond the delay time for a direct line-of- sight path,

The amplitude of the delayed component was greater than that of the direct signal. In addition to field measurements, Turin carried out simulation of multipath propagation and analysis of optimal receiver characteristics for multipath conditions. A problem with the use of short pulses is that as pulse width is reduced peak power must be increased to maintain a sufficient signal-to-noise ratio, and there are practical limits to increasing peak power.

Another approach to multipath measurements involves broadband biphase pseudorandom modulation of the transmitter output and correlation of the received signal with a replica of the transmitted waveform. The use of broadband modulation supplies the needed time resolution and avoids the pak-power problem encountered when using short pulses. The RAKE technique (Price and Green, 1958; Bitzer, 1966; Barrow et al., 1969) involves the use of a tapped delay line as part of the receiving system. The appearance of the delay line and taps on circuit drawings suggests the prongs of a garden rake, and that is the basis for the name of the technique. In the investigations by Barrow et al. of multipath effects associated with tropospheric scatter at 900 MHz, the delay line had ten taps spaced by 0.1 μs and thus covered a total delay of 1 μs. The output of each tap in such a system is correlated with the received signal to obtain data on signal amplitude as a function of time delay r. The Fourier transform of the correlation functions are taken to obtain power spectral densities $V(\tau,\nu)$ where ν is Doppler frequency. Data are then displayed as three-dimensional plots showing amplitude as a function of time delay and Doppler frequency.

Cox (1973) has carried out studies of propagation at 910 MHz in the urban environment of New York City, the interest being in terrestrial mobile radio service. Some of his work in New York was carried our with a RAKE-like receiver and also presented as three-dimensional plots of signal amplitude as a function of time delay and Doppler frequency. Excess time delays up to about 10 μs were observed but a large fraction of the total signal power occurred for delays of 2 μs or less.

Wideband propagation measurements have been carried out by the Institute for Telecommunication Sciences, National Telecommunications and Information Administration (ITS/NTIA) and the U.S. Army Communications Electronics Command.

Instrumentation development and measurements on 11.8 and 27.2 km line-of-sight paths were conducted by" ITS (Espeland, Violette, and Allen, 1984). A system operating at 30. 3 GHz utilized bipbase modulation by a pseudorandom code at a clock rate of 500 MHz with code lengths of 127 or 32,767 bits. The code rate provided a time resolution of about 2 ns, and the code lengths of 127 and 32,767 bits allowed covering delay spreads of about 0.25 μs and 66.7 μs respectively, Rather than using a tapped delay line as in RAKE receivers, the clock at the receiver operates at a few Hz slower than that of the transmitter with the result that in about a one-second period all bits of the receiver code slide by the received signal. When all the ones and zeros of the two codes or words (receiver and transmitted signal) coincide, a useful output is obtained. One does not need to take the Fourier transform of the correlation function and, if the Doppler frequencies are not of very great interest, one can display signal amplitude as a function of time in a series of two-dimensional plots. In addition to the 30.3 GHz transmissions for which bit error rate (BER) was recorded, coherent CW transmissions were utilized at 11.4, 28.8, and 96.1 GHz.

Measurements emphasizing propagation studies under conditions of irregular terrain and vegetation were carried out cooperatively by ITS and the Army Electronics Command (Hufford et al., 1983; Sass, 1983). In one phase impulses lasting 340 ns were transmitted once a second at frequencies of 600, 1200, and 1800 MHz. Biphase modulation, utilizing a 150 MHz clock rate and a 5 1 1-bit code, provided a resolution of better than 10 ns and a measurable delay spread of 3.4 μs.

Results of fading measurements that were carried out to aid in designing land mobile satellite systems are given in Sec. 6.4.

6.3.2 Equalization and Diversity

Equalization is a technique for combating distortion in transmission systems, and space and frequency diversity are measures to ameliorate fading due to multipath propagation, attenuation due to rain, etc. A comprehensive treatment of these topics is not given here, but mention is made of certain aspects.

Amplitude equalization has been commonly used to compensate for distortion caused by differential attenuation of the component

frequencies of signals. For digital systems, however, adaptive transversal equalizers that compensate for both amplitude and delay distortion have been used. These equalizers utilize tapped delay lines much like those used in RAKE receivers. Figure 6.13 shows a form of an adaptive equalizer. The signals having delays indicated by $x(t \pm iT)$ feed into amplifiers having gains which can be adjusted to provide an optimum output h(t). The use of such equalizers is not restricted to broadband systems. A definitive tutorial paper on the subject (Qureshi, 1982) refers to the use of adaptive equalizers for combating distortion on lines that are used to transmit digital data at 2400 bps.

Space diversity, which can be accomplished with antenna spacings of one-half wavelength, has received attention as a means of combating fading (Jakes, 1974). Signals from arrays of antennas may be combined by maximal ratio diversity combining which is coherent and adaptive, Yeh and Reudink (1982) have pointed out the virtue of coherent space diversity combining in dealing with interference and advocated its use to achieve efficient spectral utilization. The advantage with respect to interference is that the wanted signals combine coherently while interfering signals combine incoherently. The advantage of space diversity in mobile systems must be weighed against the increased complexity and cost of antenna arrays and circuits for coherent combining.

Spread spectrum systems, described in the following Sec. 6.3.4, provide frequency diversity. Copper and Nettleton (1983) state that a margin of 20 to 30 dB is typically required for multipath fading in narrowband systems, whereas a margin of about 2 to 3 dB may be needed for spread spectrum systems. The basis for the improvement is that all of the frequencies within the broad bandwidth of spread spectrum systems do not fade simultaneously.

The concept of coherence bandwidth is pertinent to consideration of frequency diversity. It was pointed out by Jakes (1974) that electric field intensity under multipath conditions may be represented in the following reamer.

$$E_z(\omega,t) = E_o \sum_{n=1}^{N} \sum_{m=1}^{M} C_{nm} \cos\left(\omega t + \omega_n t - \omega T_{nm}\right) \qquad (6.47)$$

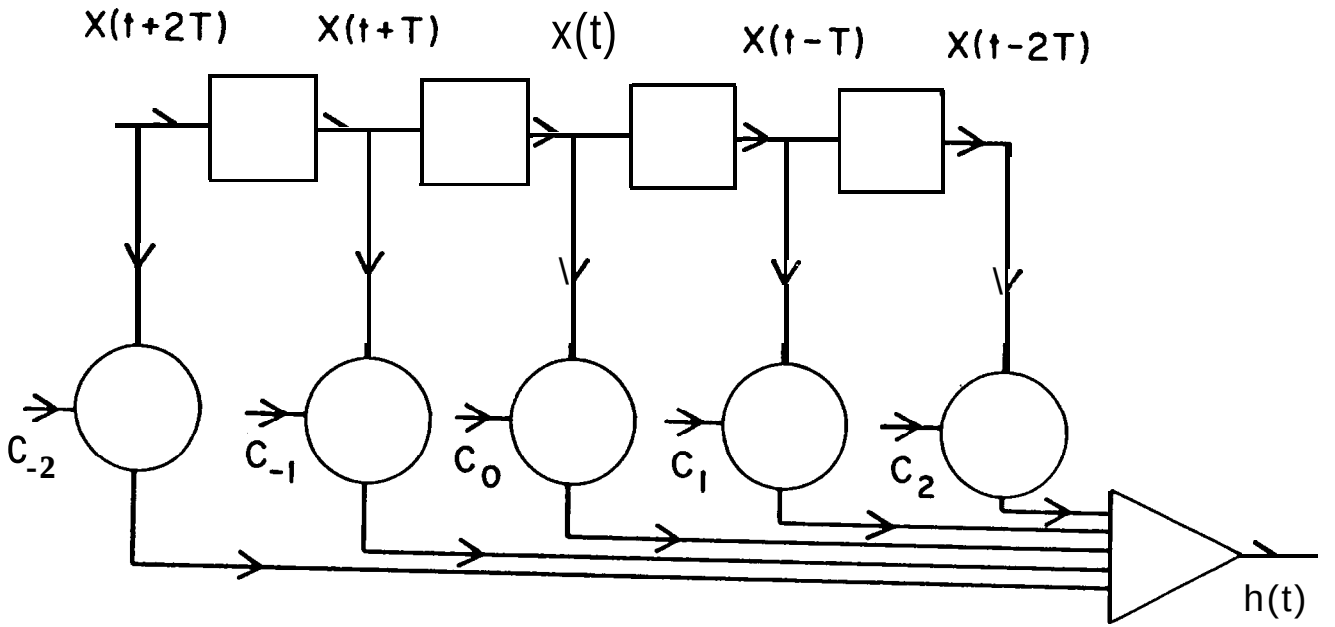

Figure 6.13. Form of adaptive equalizer.

The quantities E_z and E_o are electric field intensities, ω_n is Doppler frequency, and T_{nm} represents time differences between the multipath signal components. The phase ωT_{nm} typically has a value of hundreds of radians, and it can be readily appreciated that a rather small change in angular frequency ω results in a significant change in phase. "The analysis by Jakes shows that the coherence bandwidth B_{coh} for the envelope correlation to reach a value of 0.5 is given by

$$B_{coh} = 1/(2\pi\sigma) \tag{6.48}$$

where σ is the time delay spread of the multipath components, as determined by the techniques of Sec. 6.3.1. If σ is 1 μs, for example, B_{coh} is 159 kHz, and if σ is 0.25 μs B_{coh} is 637 kHz. Coherence bandwidths typically vary between about 100 kHz and 1 MHz. Systems having significantly wider bandwidths can provide beneficial frequency diversity.

6.3.3 Narrowband Analog Systems

It is Sec. 6.4 that is devoted specifically to land-mobile systems, but we note here that only a very limited spectrum may be available for these systems. It is important, therefore, to use this spectrum efficiently. Whereas conventional land-mobile systems may utilize. a bandwidth of 30. kHz for an audio channel, employing FDMA (frequency-division multiple access), an effort is being made to utilize bandwidths as low as 5 kHzor lower for the same purpose in land-mobile satellite service. Second-generation land-mobile satellite systems may use narrowband digital techniques to acheive operation with 5 kHz channels, but a number of the parties that have applied for licenses for first-generation systems plan to use analog single-sideband systems. In t is Sec. 6.3.3, we describe an antimultipath technique that appears to have merit for such service. For a more nearlycomplete treatment of single-sideband operations see Sec. 10.6. Sec. 6.3.4 mentions digital narrow-band operations briefly and points out that a pilot-tone technique may be advantageous for digital as well as analog narrow-band systems.

One of the possible modulation techniques for audio communication over land-mobile systems is companded single sideband. This technique is efficient in use of bandwidth, and commanding reduces the signal-to-noise ratio that would otherwise be required (Sec. 10.6). The use of a transparent tone-in-band (TTIB) pilot tone with feed-for-wad signal regeneration (FFSR). has been investigated as a meansof improving speech quality in mobile radio links subject to fading (Bateman et al., 1985). A notch filter removes a small portionof the audio signal and a tone then occupies the portion removed. The tone-in-band technique contrasts with the tone-above-band approach. FFSR utilizes identical delays in parallel signal and control (pilot-tone) paths to provide improved operation in fading environments. Let the signal at a point in the receiver be represented by

$$y(t) = E\, r(t) \cos [\omega_1 t + \omega_p t + \phi(t)] + S\, r(t) \cos [\omega_1 t + \omega_s t + \phi(t)] \tag{6.49}$$

with r(t) and $\phi(t)$ representing unwanted amplitude and phase modulations. E represents the pilot tone, and ω_p is its angular frequency; S represents the signal, and ω_s is its angular frequency. The audio signal and pilot tone then pass through parallel paths characterized by identical delays and a control signal

$$n(t) = \frac{C}{r(t)} \quad \text{Cos}\,[\omega_0 + \phi(t)] \tag{6.50}$$

is developed in the control path, with C a constant and ω_c another IF frequency. Mixing the audio and control signals then results in

$$y_e(t) = \frac{SC}{2} \cos [\omega_s t + (\omega_1 - C\, d_0) t\ ] \tag{6.51}$$

and, if $\omega_1 = \omega_0$, the desired audio signal is recovered. This technique requires that the frequency of the audio signal and the fading frequencies be separable. As pointed out in Sec. 6.4, such separation appears to be possible as the maximum fading frequency canbe expected to be in the orderof 150 Hz for carrier frequencies near 850 MHz (Vogel and Smith, 1985).

6.3.4 Narrowband Digital Systems

A pronounced trend towards digital transmission is taking place, and considerable attention is directed towards Integrated Services Digital Networks (ISDN's). A related development for our purposes is that considerable effort is being devoted to achieving near toll quality digital speech at 4800 bps, utilizing 5 kHz channels. Research has been carried out at the Georgia Institute of Technology (Barnwell, i 985), the University of California, Santa Barbara (Gersho, 1985), the Jet Propulsion Laboratory (Tomes, 1985; Simon, 1985; and Divsalar, 1985), and at General Electric (1985). Pilot-tone techniques similar to those mentioned in Sec. 6.3.3 for companded single-sideband systems are being considered. General Electric has analyzed both TTIB (Transparent-Tone-In-Band) and TCT (Tone-Calibrated Technique) measures and has asserted that TCT is more bandwidth efficient than TTIB. Linear predictive coding (LPC) is discussed by Townes as one of the narrowband techniques of interest. A description of the various coding methods is outside the scope of this report but persons working with link design and propagation effects should be aware of the work that is going on in this area.

6.3.5 Spread-spectrum Systems

The frequency diversity provided by broadband systems was referred to in the previous Sec. 6.3.2. Broadband systems which achieve their bread bandwidth by use of a signal other than the information being transmitted are defined as spread-spectrum systems. Such systems can be useful for conducting multipath measurements; the systems described in Sec. 6.3.1, other than the narrow-pulse systems, are spread-spectrum systems. Also the Global Positioning System (See.6. 7) is a spread-spectrum system. Spread-spectrum systems are also useful for communication purposes.

Shannon's law shows the roles of bandwidth B and signal-to-noise ratio S/N in determining communication capacity as indicated by

$$C = B \log_2 (1 + S/N) \tag{6.49}$$

where C is the maximum theoretical communicant ion capacity in bits

per second. The value of C given by the equation can not be reached in practice, but the expression correctly indicates that a certain capacity can be achieved by using a high value of S/N and a low value of bandwidth B or vice versa. Spread-spectrum systems utilize a large bandwidth B and therefore operate with a low signal-to-noise ratio. They employ bandwidth expansion factors typically in the order of 100 to 1000 (ratio of transmission bandwidth to signal bandwidth),

The principal ways of spreading the frequency spectrum beyond that of the information content are use of direct sequence (DS), frequency hopping (FH), time hopping, and FM chirp techniques (Dixon, 1976). Attention is given here to the DS and FH techniques. By direct sequence, reference is made to modulation of the carrier by a code sequence. The most common technique is to use 180 deg biphase phase shift keying. The RF bandwidth B after modulation at a 10 Mbps code rate, for example, is 20 Mbps. If the data bandwidth in this case is 20 kbps, the ratio of bandwidths is 2000 or 33 dB. This ratio is referred to as processing gain (PG). Thus

$$PG = 2R_c/R = B/R \tag{6.50}$$

where R is the data bit rate and R_c is the code bit rate. Processing gain B/R relates carrier signal-to-noise ratio C/X and energy per bit to noise power density ratio E_b/N_o after demodulation by

$$E_b/N_o = (C/X)(B/R) \tag{6.51}$$

Assuming, for example, that an E_b/N_o ratio of 10 is needed and that B/R is 2000, C/X can be 0.005, corresponding to the signal being buried in noise, and the needed value of E_b/N_o can still be achieved. Figure 6.14 illustrates power spectra of data and spread signals in spread-spectrum systems. One form of a direct sequence spread-spectrum system is shown in Fig. 6.15. Here the carrier is modulated by the information to be conveyed before being modulated by the code sequence. An alternative procedure is to modulate the code sequence by the information. At the receiver a heterodyne arrangement is shown for obtaining the correlation bvetween the code modulated carrier and the receiver code. The signal appears as modulation of the IF frequency at the input and output of the IF amplifier. The demodulation process recovers the narrowband

baseband signal. Interference or a signal carried by a different code appears as broadband noise at the output of the mixer, and only a small fraction of this noise passes through the IF amplifier and appears at the demodulator output.

Spectrum is a valuable resource, and it might appear that spread-spectrum systems are wasteful of bandwidth. A major virtue of spread-spectrum systems, however, is that a number of users can employ the same frequency band at the same time by using different codes, The procedure for doing so is referred to as code division multiple access (CDMA). Such CDMA systems provide privacy, but not complete security, as well as freedom from mutual interference for multiple users of the same bandwidth. A principal reason for discussing spread-spectrum systems here, furthermore, is that they constitute a means for combating multipath fading (Sec. 6.3. 2). Also some spread-spectrum satellite systems are in use, and propagation effects encountered by such systems deserve consideration. An advantage of CDMA for mobile communications is that each user can be given a code and allowed to enter the system freely, up to some number. Protocol and network management functions can be reduced to a bare minimum as it is not necessary for users to request and receive channel assignments.

RAKE-type receivers, using a tapped delay line as described in Sec. 6.3.1, have a plication to spread-spectrum systems (Turin, 1980; Proakis, 1983). They are used for selecting, combining, and/or weighting the individual multipath components to provide the optimum signal-to-noise ratio much as for adaptive equalizers (Sec. 6.3 .2). For direct sequence spread-spectrum systems to function, close synchronization must be maintained between the transmitter and receiver. The simplest technique for providing synchronization involves the use of a sliding correlator such as that mentioned in Sec. 6.3.1. The sliding correlator operates with a code sequence that has a rate slightly different from that of the transmitter so that the two sequences slip in phase with respect to each other initially but lock in phase when the point of coincidence is reached. In some FH systems no synchronization of the mobile units is required (Cooper and Nettleton, 1978).

Further attention is given to spread-spectrum systems in Sec. 10.7.

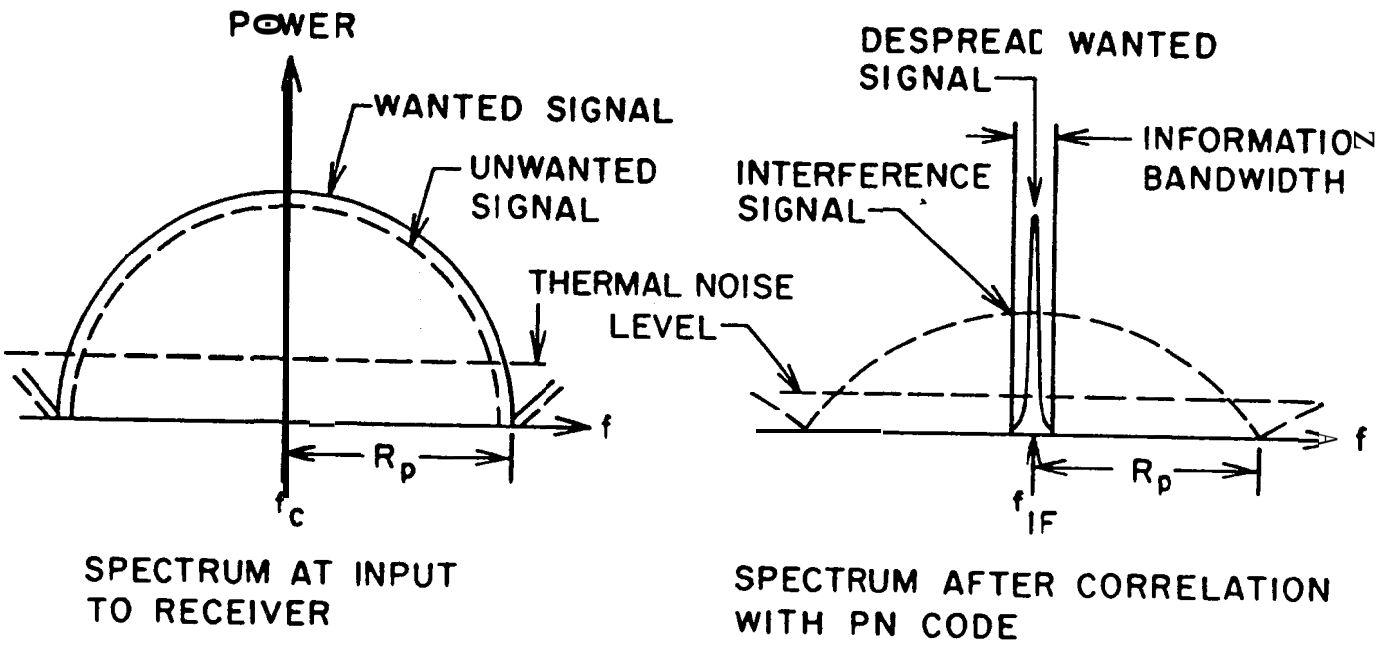

Figure 6.14. Power spectra of wanted and unwanted signals in PN spread-spectrum system.

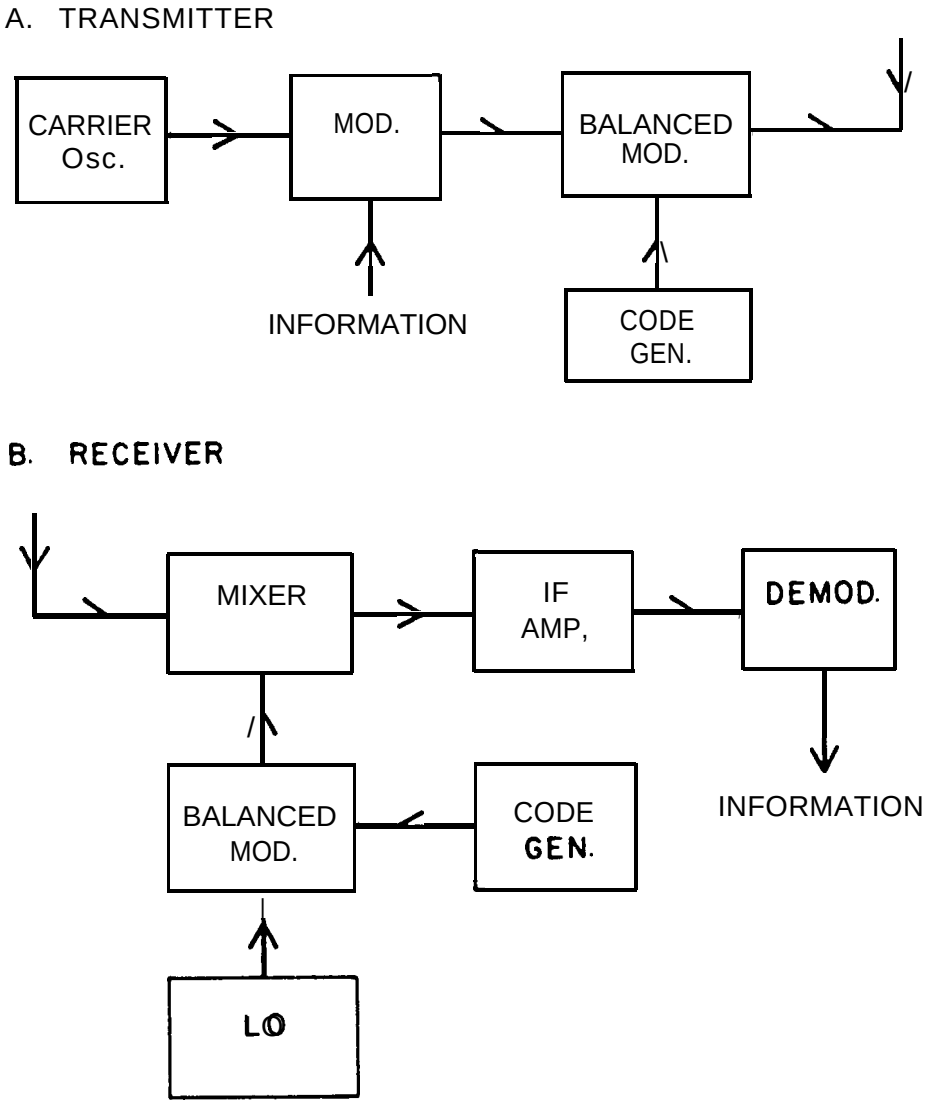

Figure 6,15. Block diagram illustrating direct-sequence spread-spectrum system.

6.4 LAND-MOBILE SATELLITE SYSTEMS

NASA, with the Jet Propulsion Laboratory playing a major role, has been actively carrying out programs to facilitate the implementation of a land-mobile satellite system since about 1980. The concept of a Land Mobile Satellite Service (LMSS) was described by Knouse (1980), and an early design of an LMSS system was prepared by Naderi (1982), Since the beginning close cooperation has taken place between NASA and the Canadian Department of Communications, and Canada has an active Canadian Mobile Satellite program, MSAT (Boudreau and Barry, 1983). In 1985 interest in land-mobile satellite service intensified. A Propagation Workshop on MSAT-X, an experimental program to obtain needed data and develop techniques (Weber and Naderi, 1983), was held at JPL on Jan. 30 and 31, 1985. Industry has shown strong interest, and twelve companies have applied to the FCC for licenses to offer land-mobile service. A Mobile Satellite Industry Briefing at JPL in Nov., 1985 was attended by a large number of investigators and representatives of the companies who applied for licenses. At the time, the FCC had not indicated whether authorization would be granted for operation in portions of the 806 to 890 MHz band or for the L band (about 1500 to 1700 MHz). A July 28, 1986 decision favored the L band, but at the time of writing no licenses have been granted. The companies that have applied have plans for first-generation systems, which will tend to have relatively simple antennas, with many of the companies planning to use analog companded single-sideband modulation. JPL is concentrating attention on research and development on second and third generation systems which may employ large multibeam antennas on the spacecraft and sophisticated digital modulation techniques.

An earth-space path may experience specular reflection and diffuse scatter and resulting fading, as discussed in Sec. 6.2, but fixed earth stations can be designed to minimize such problems. Mobile satellite services are vulnerable to fading from the above causes for two principal reasons. One is that they must operate in a large variety of locations which cannot be selected or prepared in advance. A second major factor contributing to fading is movement of the vehicle. No matter how reliable the signal may be when the vehicle is stationary and in a favorable location, fading becomes a potential problem for a moving vehicle.

Certain measures can be taken to minimize fading. The use of directional antemas which discriminate against reflected rays is one important means. This approach is most effective in the case of satellites at rather high elevation angles, as contrasted to terrestrial services and low-angle satellites. Circular polarization has the favorable features of relatively low reflection coefficients, compared to horizontal polarization, and the fact that reflected rays above the Brewster angle tend to be predominantly cross polarized with respect to incident rays. As receiving antennas are designed for the transmitted polarization, they are insensitive to the orthogonal or cross polarized components of the reflected rays. Thus multipath fading, resulting from interference between direct and reflected rays, is minimized.

Specular reflection and diffuse scatter continue to be of concern to land mobile satellite operations, but certain measurements reported later in this section have tended to shift emphasis to shadowing by roadside trees, especially in the case of two-lane roads. In canyon country or mountainous areas, shadowing by terrain may be important. On broad interstate highways, specular reflection and diffuse scatter may predominate. Effects of vegetation were considered in Sec. 5.3, but the results to be mentioned in this section refer to conditions simulating those of earth-space paths. The situation in this case is quite different from that for propagation from one point to another on the Earth's surface, where the paths are close to horizontal and involve propagation through and/or diffraction over trees as in Fig. 5.2. For earth-space paths the geometry is like that shown in Fig. 6.19.

Measurements were made of signal intensities of transmission from the ATS-6 satellite to mobile receivers at 860 MHz and 1550 Mhz in a number of cities in the United States (Hess, 1980). The data reported were primarily from Denver. The excess path loss for 90 percent spatial coverage for 90 percent of the time for urban areas is about 25 dB and is quite insensitive to frequency. The statement is made that a comparable value for suburban/rural areas is under 10 dB. The probability density of signal intensity is found to be different from that of the Raylei gl distribution. Another study (Brisken et al., 1979) using ATS-1 and ATS-6

satellites determined that ground-reflection multipath and ignition noise affected satellite communications less than terrestrial mobile communications.

Canadian studies of propagation effects on land-mobile satellite service have been described by ButterWorth and Mott (1983). A signal source in a helicopter was used in some of their studies. Vogel and Torrence (1984) have carried out measurements of signals received from balloons launched from the NASA high-altitude balloon facility at Palestine, Texas in October, 1983 and January, 1984. Table 6. 1 shows some of their results. Shadowing by trees appeared to play a major role in causing the low signal levels shown in the table in the 99 percent column. In November, 1984, another balloon experiment was carried out, this time utilizing a balloon dedicated to the purpose (Vogel, 1 985). A summary of propagation considerations related to land-mobile service was prepared by Vogel and Smith (1 985).

Some results of measurements made in Canada and Texas are illustrated in Fig. 6.16, Such curves typically consist of two portions, one with the signal dropping rather slowly and the other with the signal dropping more rapidly. The first portion is believed to represent Rician fading, and the second portion is believed to due to lognormal fading caused by shadowing by trees (Butterworth, 1985; Stutzman, 1985). Data in terms of K values (ratio of direct power to multipath power) obtained by Vogel and interpreted by Smith (1986) are shown in Fig. 6.17.

The measurements using helicopters and balloons simulated earth-space propagation. Another useful method of simulation is by use of hardware. The Jet Propulsion Laboratory has designed and implemented an end-to-end hardware simulation of mobile satellite communication links. The simulator includes a propagation path simulator and interference transmitters for investigating propagation effects and interference (Davarian, 1 987). Also included are provisions for studying Doppler effects (see following paragraph), band limiting, satellite nonlinearity, and thermal noise.

Table 6.1 Signal Power in dB Relative to Mean as a Function of Elevation Angle θ and Probability, Transmitter in High-altitude Balloon (Vogel, 1984).

Elevation Angle	Probability (percent)		
(degrees)	50	90	99
10<θ<3s	-1.0	-7.0	-18.0
10<6 <15	-1.0	-9.0	-20.5
15 < θ <20	-1.0	-8.0	-18.5
20 < θ < 25	-1.5	-9.8	-20.3
25 < θ <30	-0.8	-2.2	-8.2
30 < θ <35	-0.5	-1.2	-4.5

For 10 { θ <35 and a probability of 99 percent, for example, the signal power is within 18 dB of the mean for 99 percent of the time, or more than 18 dB below the mean for 1 percent of the time.

Attention will now -be given to the fading rate encountered under multipath conditions. Consider the situation depicted in Fig. 6.18, where scatter is received predominantly from a particular region. In this case, for a vehicle moving with velocity v, the frequency of the direct signal experiences a Doppler shift f_d given by

$$f_{d_1} = \frac{v_r}{\lambda} = \frac{V_r f}{c} = \frac{v \cos\theta \, f}{c} \qquad (6.55)$$

where v_r is the component of velocity parallel to the path, θ is elevation angle, c is the velocity of light, and f is the transmitted frequency. The signal component scattered from the dominant scatterer, however, experiences a shift f_{d_2} given by

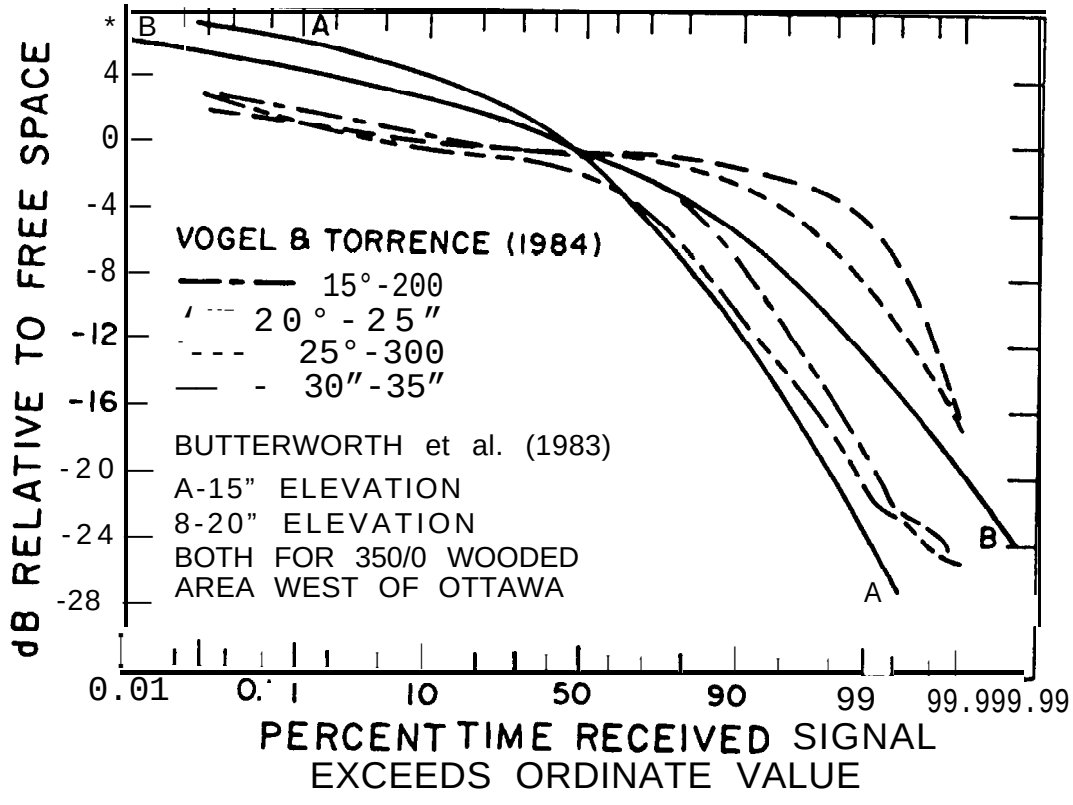

Figure 6.16, Statistical characteristics of simulated land-mobile signals.

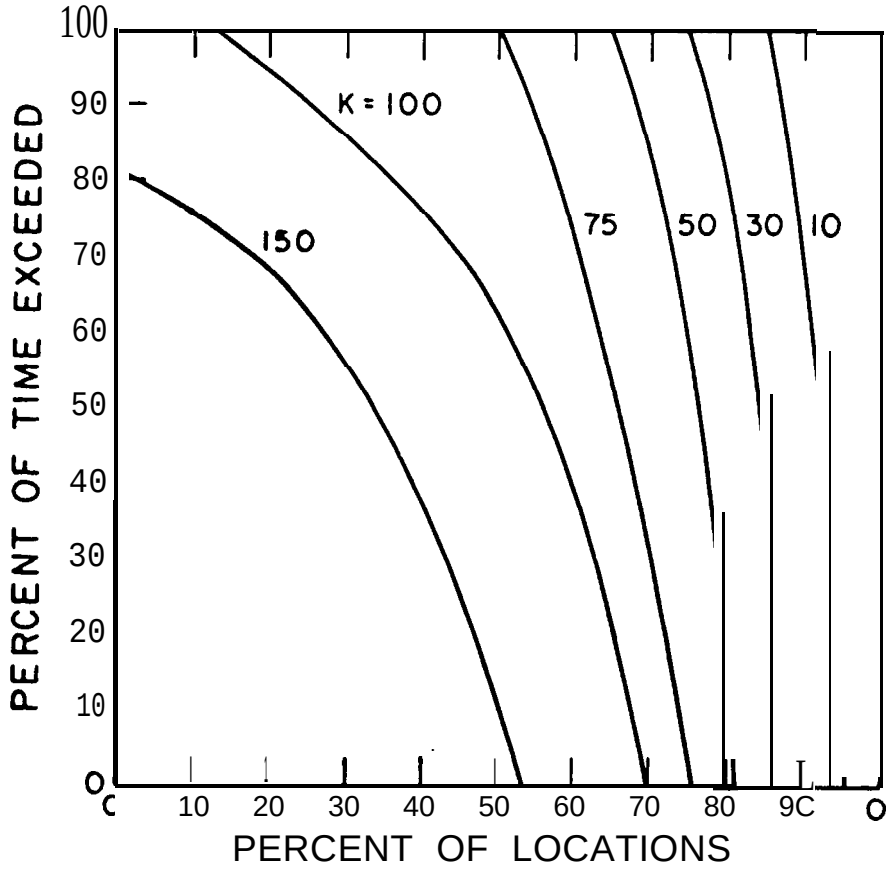

Figure 6.17. K values (ratio of power in steady component of signal to random component) as a function of location and time. Data by Vogel, interpreted by Smith (1986). Example: A K value of 75 is exceeded for about 74 percent of the time in 60 percent of the locations.

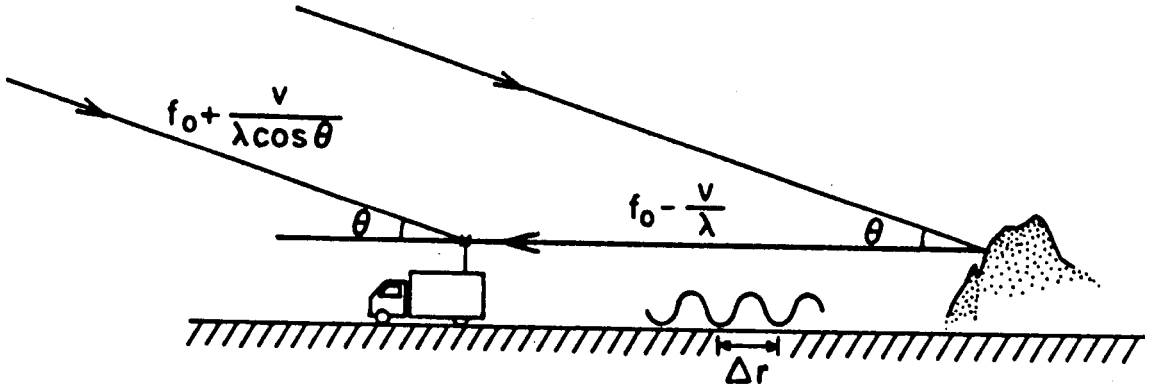

Figure 6.18. Doppler frequencies of land-mobile satellite signals received by moving vehicle.

$$f_{d_2} = -\frac{v f}{c} \tag{6.56}$$

so that the difference in the two Doppler shifts Af is

$$\Delta f = f_{d_1} - f_{d_2} = \frac{Vf}{c} (\cos\theta + 1) \tag{6.57}$$

In the limiting case for which $\theta = 0^{o}$

$$Af = 2vf/c = 2v/\lambda \tag{6.58}$$

As in general $f_d = (1/2\pi)\, d\phi/dt$ where ϕ is phase

$$\phi = 2\pi \int \Delta f\, dt \tag{6.59}$$

where ϕ is the difference in phase between the two signal components. It is evident that ϕ varies linearly with time so that at one instant the two signals reinforce each other and at another time they interfere destructively, with the result that signal amplitude varies at the frequency Af. For v = 100 km/h and f = 850 MHz, Δf = 157 Hz from Eq. (6.58). Thus an estimated maximum frequency of fading is 157 Hz. A standing wave of field intensity exists along the roadway with peaks in the standing wave pattern spaced $\lambda/2$ apart in the limiting case or $\lambda/(1 + \cos\theta)$ in general. The above discussion of fading rate follows that by Vogel and Smith (1985).

Measurements of shadowing on tree-lined roads and by single trees have been made by Vogel and Goldhirsh and coworkers at Wallops Island, Virginia and in Maryland using transmitters in drone aircraft or helicopters (Vogel and Goldhirsh, 1986; Goldhirsh and Vogel, 1987). Attenuations of about 2 dB/m at 869 MHz and 2.8 dB/m at 1500 MHz, with total attenuations of 10 to 20 dB, were recorded. The above attenuation constants of 2 to 2.8 dB are larger than those indicated by the use of $\alpha = 0.2\, f^{0.2} d^{0.6}$ of Chap. 5. Note, however, that the two situations (Figs. 5.2 and 6. 19) are quite different. Most recently the same parties obtained data from canyons in Colorado showing that specular reflection from canyon walls caused fluctuations of ±3 dB (Vogel and Goldhirsh, 1988).

Other possible propagation and environmental effects on land-mobile service include ionospheric scintillation, man-made noise, and multipath limitations on transmission at high data rates.

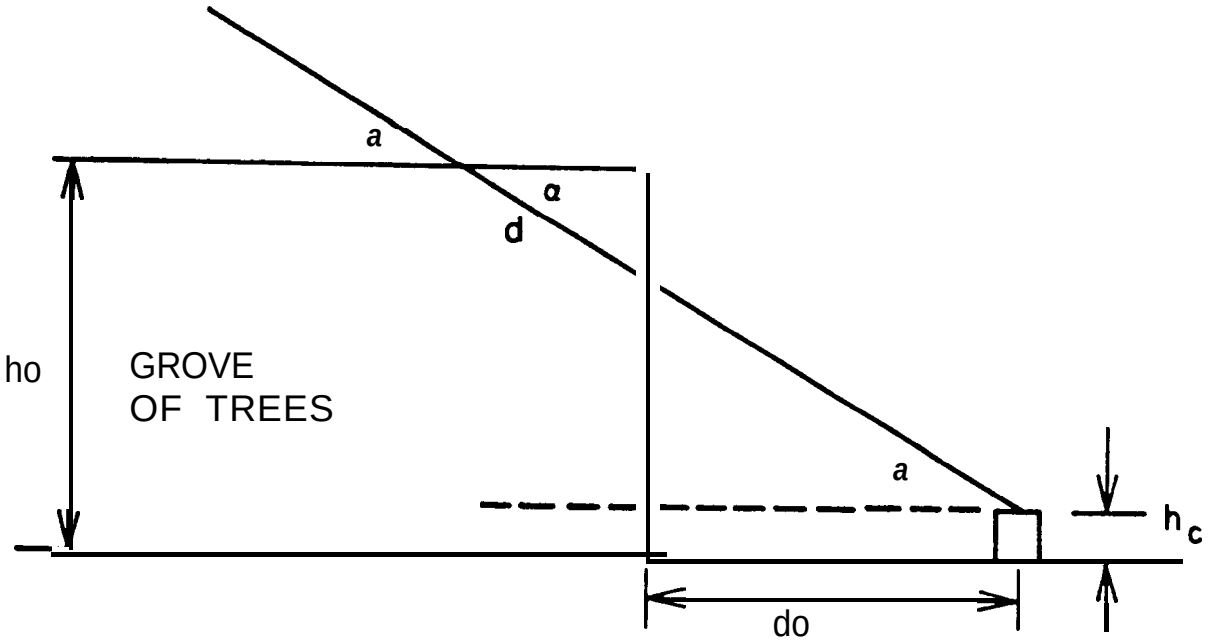

Figure 6.19. Idealized geometry for interception of satellite signal by grove of trees. (Applies to idealized single trees as well as grove).

Extrapolating from data given for 137 MHz (CCIR, 1 986i), Smith (1986) estimated that at middle latitudes like that of Hamilton, MA about 2 dB peak-to-peak scintillation might occur for about 2 percent of the time at night at frequencies like 869 and 1500 MHz, At latitudes like that of Goose Bay, Labrador (or southern Alaska) such scintillation might occur for 7 percent of the time, and at latitudes like that of Narssarssuak, Greenland (or northern Alaska) scintillation of this magnitude could occur for 45 percent of the time. For man-made radio noise CCIR Report 258-4 (CCIR, 1986 j) gives a formula for noise figure, $F_{ar}e$, of c - d log f, with f in MHz for 0.3 to 250 MHz. Values of c and d are given for business, interstate highways, and rural areas. Using the expression beyond its stated limit to obtain an estimate of values for higher frequencies gives noise temperatures as shown in Table 6.2.

Table 6.2. Noise Temperatures for Man-made Noise (Smith, 1986).

Area	c	d	Noise Temperatures (K) 869 MHz	1500 MHz
Business	76.8	27.7	100	22
Interstate Highways	73.0	27.7	42	9
Rural	67.2	27.7	11	2.4

Propagation effects on satellite mobile service are treated in Report 884-i on maritime mobile service (CCIR, 1986e) and Report 1009 on land mobile service (CCIR, 1986f), both in Volume V, Recommendations and Reports of the CCIR, 1986. In 1982 CCIR Report 884 dealt with both maritime and land mobile service. Volume VIII-3, Recommendations and Reports of the CCIR, 1986 also deals with satellite mobile service, including aeronautical, land, and maritime services. It emphasizes aspects other than propagation. In 1982 these satellite services were treated in sections of one larger Volume VIII devoted to Mobile Service.

6.5 MARITIME-MOBILE SATELLITE SYSTEMS

Maritime-mobile systems must contend with reflection and scatter from the surface of the oceans and seas. Serious ionospheric scintillation may be encountered at geomagnetic latitudes between about 20 deg N and S, especially at frequencies near 1.5 GHz and lower as reported in Sec. 2.6.4. Propagation at low elevation angles tends to present problems over water as well as over land, and serious effects have been reported and analyzed (Fang, Tseng, and Calvit, 1982; Fang and Ott, 1983; CCIR, 1986g).

The electric field intensity at a maritime-mobile receiving antenna, due to signals transmitted from a satellite, is the vector sum of components associated with the direct wave from the satellite, a specularly, coherently reflected wave, and a diffusely, incoherently scattered wave. The magnitude of the reflection coefficient for the specularly reflected wave is decreased below that for a smooth surface by a roughness factor which is described in Sec. 6.2.4 and shown specifically by Eq. (6.28). As the specular reflection coefficient decreases due to increasing roughness, diffuse scatter becomes important. Diffuse scatter is said to be dominant in practice, with normal sea conditions in most areas, but specular reflection plays a role in at least relatively smooth seas.

In CCIR Report 884-1 (CCIR, 1986e), it is assumed that a Rice-Nakagami distribution applies to the combination of a direct wave and diffuse scatter that is observed. In proposed modifications to Report 884, which however were not included in Report 884-1. models of sea surface characteristics as a function of wind speed are used to provide values of the C/M (carrier-tomultipath) ratio in dB versus wind speed for vertical, circular, and horizontal polarization. For small elevation angles, vertical polarization gives a better C/M ratio than circular or horizontal polarization. For large elevation angles, the reflected wave may have predominantly the orthogonal or cross polarization with respect to the circular polarization that is transmitted. The antenna is designed for the transmitted polarization and it discriminates against the orthogonal polarization with the result that circular polarization may have an advantage over vertical and horizontal polarization at large elevation angles. Figures 6.20 and 6.21 show examples of results obtained by use of the models mentioned.

The actual results in a particular case will depend on antenna gain as a function of off-boresight angle and polarization. Figure 6.22 shows reflection coefficients for a smooth plane sea. It can be appreciated that multipath tends to be less of a problem for vertical polarization because reflection coefficients are smaller for this polarization than for horizontal polarization (Fig. 6.22), and the same statement applies for circular polarization for angles less than and not too far above the Brewster angle. Link power budgets for the maritime mobile satellite service are treated in CCIR Report 760-1 (CCIR, 1986h).

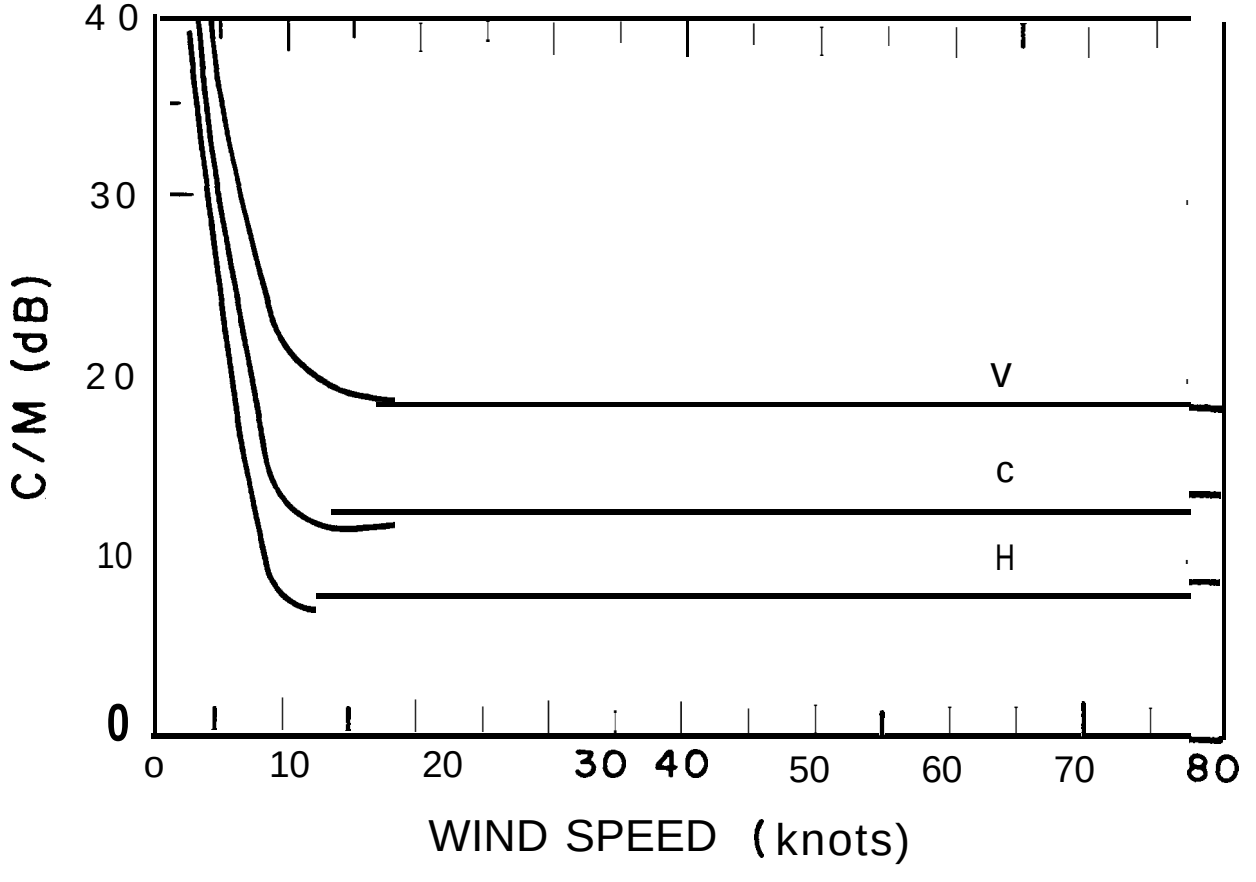

Figure 6.20. C/M ratio versus wind speed for antenna gain of 14 dB and elevation angle of 5 deg (CCIR, 1983).

On February 1, 1982. the International Maritime Satellite Organization (INMARSET) started to provide maritime service (da Silva Curiel, 1983). It took over and expanded the previous MARISAT system which commenced operation in 1976 and provided service for the Atlantic, Pacific, and Indian oceans with three MARISAT satellites. At first INMARSAT used the three MARISAT satellites, but the plan has been to use Maritime Communication Subsystems (MCS) on INTELSAT V satellites or MARECS satellites and to keep the MARISAT satellites as spares. Each satellite receives transmissions at 6 GHz from shore stations and translates them to 1.5 GHz for transmission to ships. Transmissions from ships to satellites are at 1.6 GHz and those from the satellites to the shore stations are at 4 GHz. An allowance of 4 dB for short-term fading was provided for the L-band links in the original MARISAT systems (Lipke et al,, 1977).

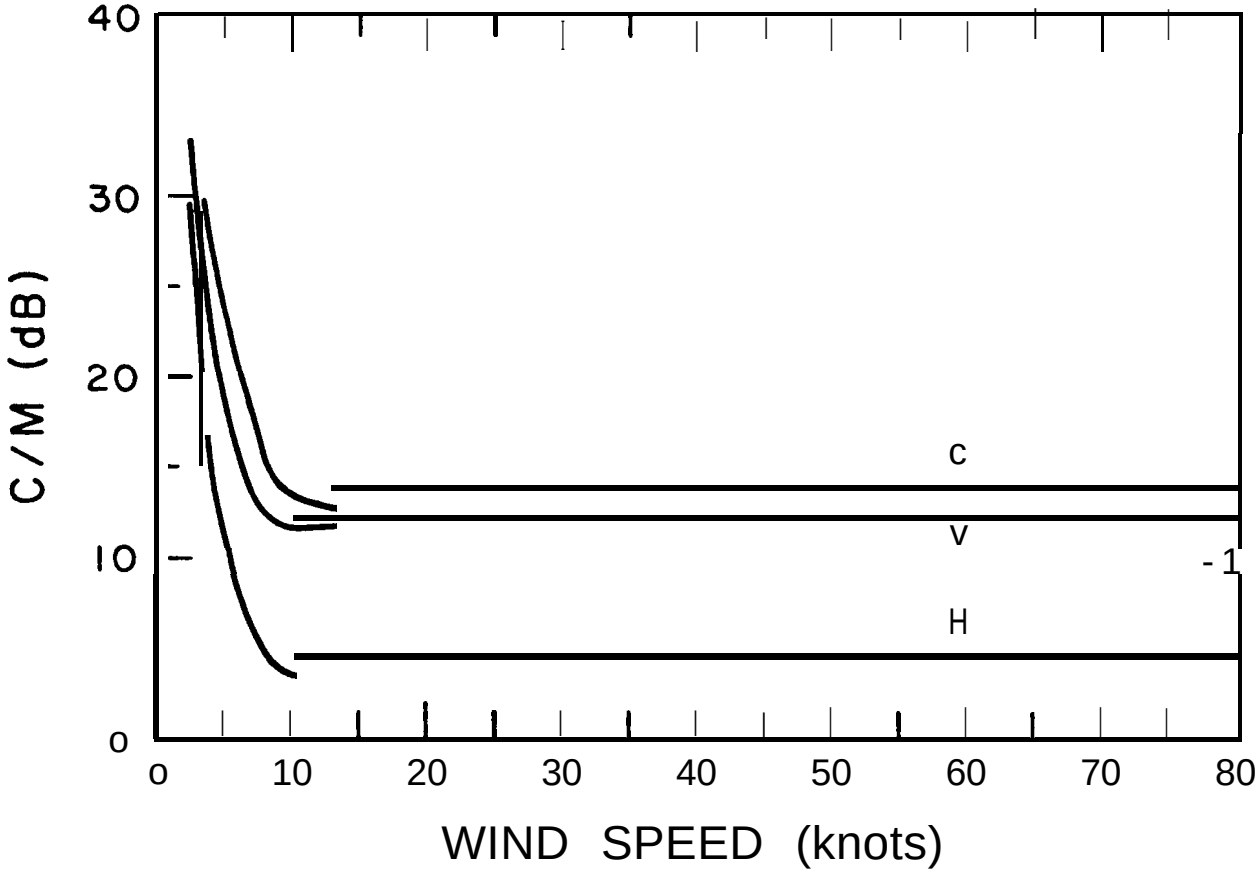

Figure 6,21, C/M ratio versus wind speed for antema gain of 8 dB and elevation angle of 15 deg (CCIR, 1983).

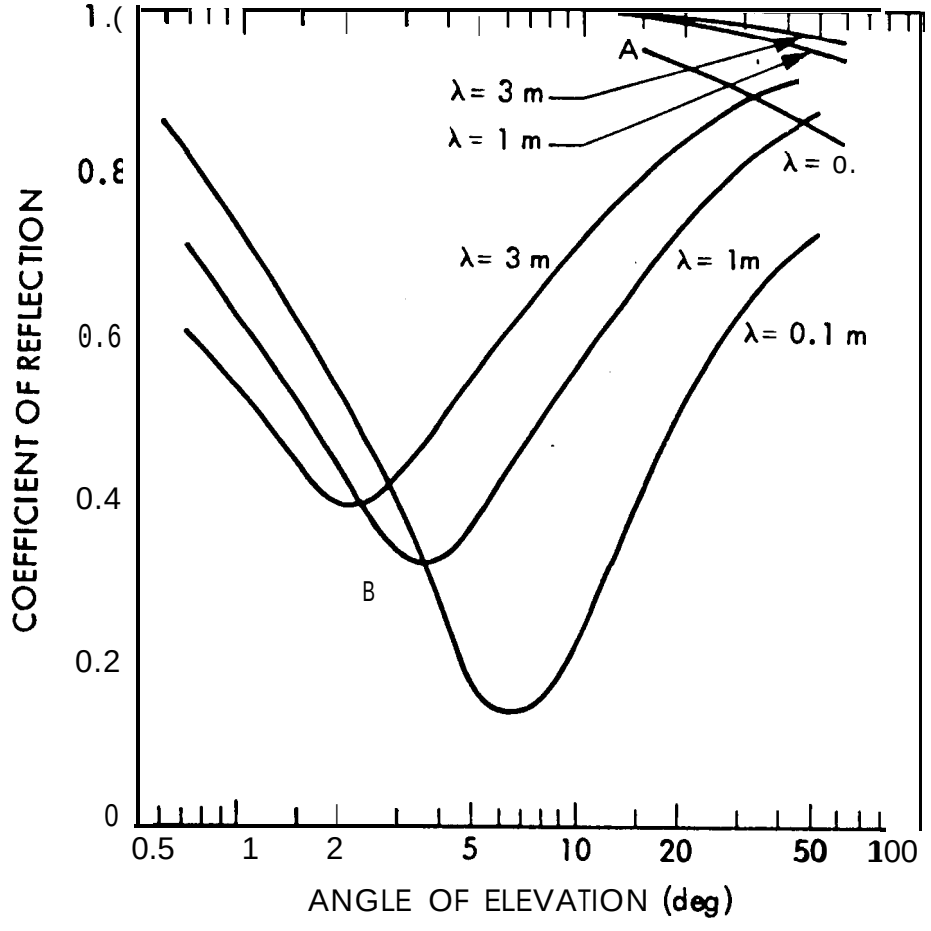

Figure 6.22. Reflection coefficients for smooth plane sea. A: horizontal ; B: vertical polarization (CCIR, ital polarization 1982).

6.6 AERONAUTICAL-MOBILE SATELLITE SYSTEMS

Because of the heights at which aircraft fly, aeronautical-mobile satellite operations involve considerations that may not be important for vehicles and ships that are confined to the Earth's surface. For surface operations, multipath propagation is of importance primarily because of the resulting fading. For aeronautical operations, however, time delays of the reflected rays with respect to the direct rays may be of importance as well. The time delay is greatest when an aircraft is directly beneath a satellite. For an aircraft at an altitude of 15 km, for example, the time delay of the reflected ray is 1 00 μs. For the north Atlantic air routes and a geostationary satellite at 30 deg of longitude, the delay times for aircraft between 8 and 17 km are between about 20 and 60 μs.

Multipath time delays may cause intersymbol interference but the time delays do not cause significant garbling of voice signals. The effect on digital transmission depends on the relative magnitude of the time delay and bit length. When the two periods are comparable, errors may arise unless remedial measures are taken. If the bit period is large compared to the propagation delay and sampling is done at the center of each bit period, problems are minimal.

For small elevation angles and aircraft heights above about 10 km, the reflection from a smooth surface is reduced by the Earth's curvature below the value for a plane earth. The factor by which the reflection coefficient is reduced is known as the divergence factor D (Beckmann and Spizzichino, 1963) and is illustrated in Fig. 6.23 for two different aircraft heights. Aircraft can range over land and sea and also over areas of ice and snow such as the Greenland ice cap and Antarctica. Reflection coefficients for such surfaces, consisting of snow which gradually changes with depth to compact snow and then to ice, are illustrated in Fig. 6.24.

Aircraft in flight pass through the maxima and minima of the interference pattern which is set up by reflection, and they experience fading which is a function of the applicable reflection coefficients. The vertical separation Δh_r between maxima of the

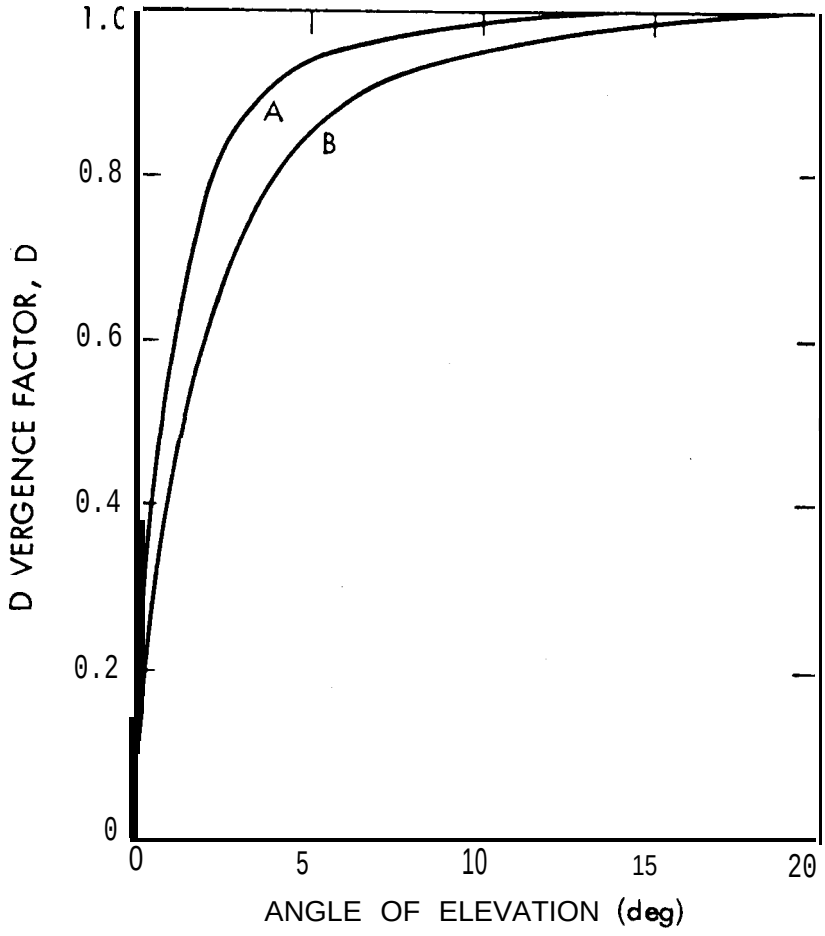

Figure 6.23. Divergence factors, D for reflection from a smooth spherical earth, A: aircraft at 3,000 m; B: aircraft at 10,000 m (CCIR, 1978).

interference pattern can be found from Eq. (6.8), assuming reflection from a plane surface, by setting

$$\frac{2\pi\Delta h_r \sin\theta}{\lambda} = \pi$$

from which

$$Ah_r = \frac{\lambda}{2 \sin\theta} \qquad (6.60)$$

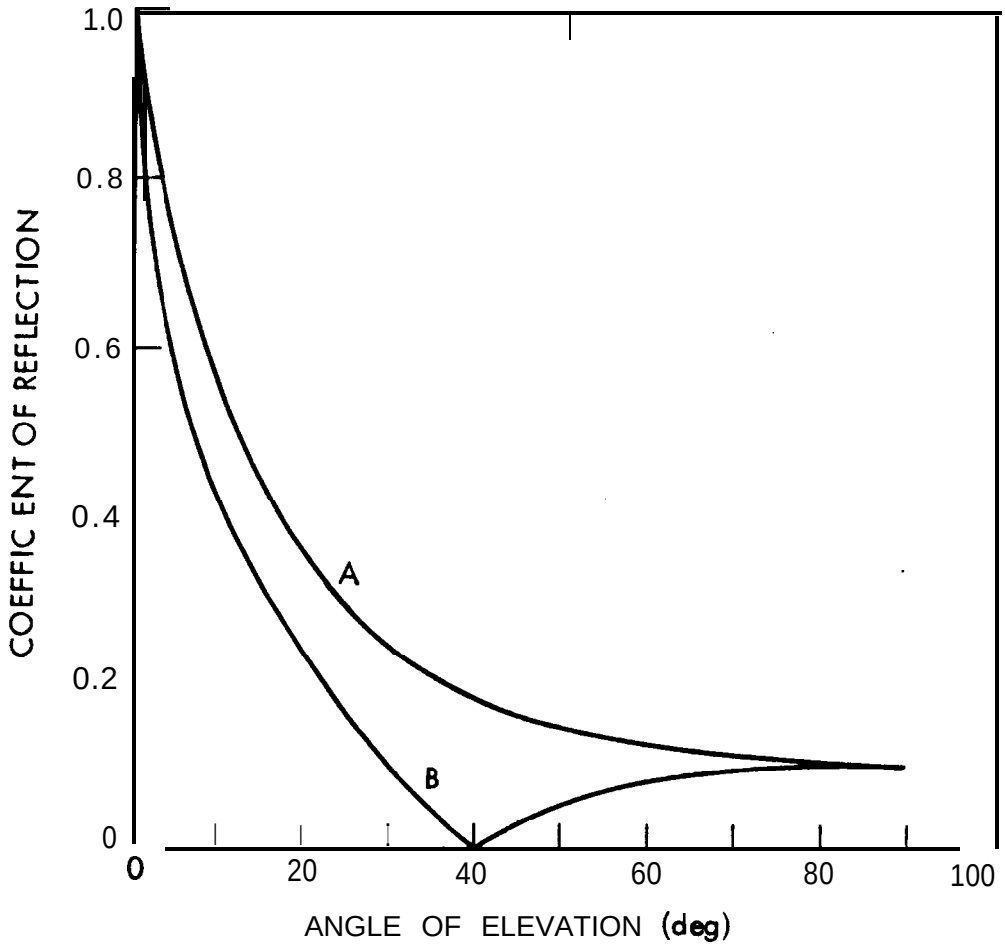

Figure 6.24. Field intensity reflection coefficients for ice caps such as those of Greenland and Antarctica. A: horizontal polarization, B: vertical polarization (CCIR, 1982).

Table 6.2 lists values of Δh_r as determined from Eq. (6.60) for various angles 9. Ascending and descending aircraft pass rapidly

Table 6.2 Vertical Separation Between Maxima of Interference Pattern,

θ (deg)	$\Delta h_r(\lambda)$
2	14.3
4	7.2
8	3.6
15	1 . 9
30	1.0
60	0.58
90	0.5

through the maxima and minima in the interference pattern. For elevation angles of about 15 deg and greater even aircraft in nominally level flight experience the full range of fading because of limited ability to maintain constant height.

In flight over water the Doppler spectrum of the sea-reflected signal introduces spectral spreading of the received signal, as a function of the elevation angle of the aircraft with respect to the origin of the reflected signal. Values of the measured Doppler bandwidth between points at. 1/e of the peak amplitude for L-band transmissions from ATS-5 are shown in Fig. 6.25.

An AEROSAT satellite system specifically designed for aircraft communciations has been proposed but never funded, but at the time of writing" the application of satellites to communication with aircraft appears imminent (Sue, 1987). Volumes VIII-1, VIII-2, and VIII-3, Mobile Services, Recommendations and Reports of the CCIR. 1986 include a large number of reports that provide information pertinent to mobile communications, including mobile-satellite communications. Although Report 505-2 (CCIR, 1978) was not updated and included in subsequent cycles of publication, this writer found it to be a useful- report. Several of the illustrations used in this chapter appeared in Report 505-2 and then in Report 884 (CCIR, 1982).

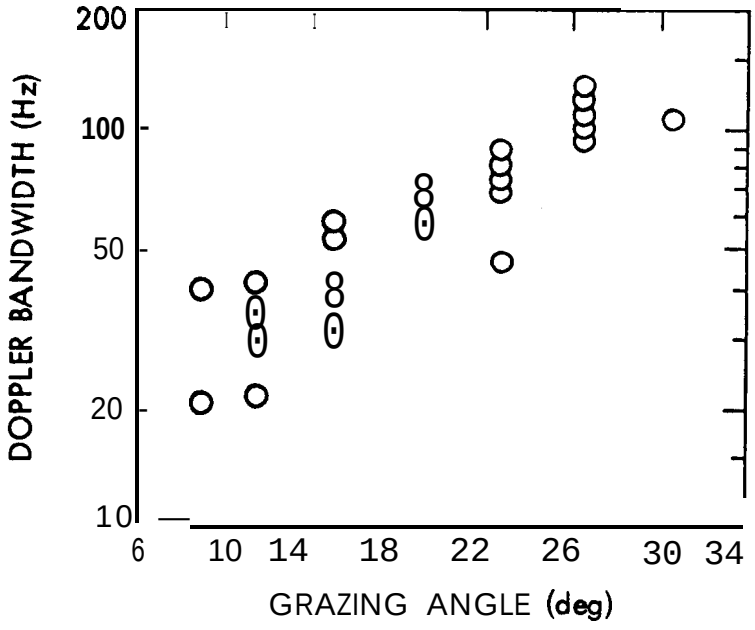

Figure 6.25. Doppler bandwidth as a function of elevation angle, based on 1550 MHz transmissions from the ATS-5 satellite to a 707-type aircraft (CCIR, 1982),

6.7 THE NAVSTAR GLOBAL POSITIONING SYSTEM

The three previous sections have involved consideration of multipath effects that may be important to the three categories of land, maritime, and aeronautical mobile communications services. In addition, the effects are pertinent to radionavigation systems, including the NAVSTAR Global Positioning System (GPS) (Milliken and Zoner, 1978). The system provides three-dimensional position and velocity information to mobile or fixed receivers anywhere in the world whether on land or sea or in the air. Original plans called for 24 satellites in 12-hour orbits at an altitude of 20,183 km in three orthogonal planes (eight in each plane). Budgetary considerations have required a change to operation with a total of 18 satellites (Book, Brady, and Mazaika, 1980). Signals are transmitted at two L-band frequencies, 1575.42 and 1227.60 MHz, to permit correction for ionospheric time delay. The satellites carry precision cesium clocks, and if the user has a precision clock signals from three satellites are sufficient to determine position. A fourth satellite is required for most users, however, who must have a clock of specified accuracy but not a truly precision clock. Each of the two L-band frequencies is a multiple of a 10.23 MHz clock frequency. In particular 154 x 10.23 = 1575.42 and 120 x 10.23 = 1227.60. By making measurements of pseudo range to the four satellites, four equations can be formulated and solved for the four unknowns consisting of three position coordinates and the offset between precision GPS time and time as indicated by the user's clock. The term pseudo range is used because the originally measured quantities are sums of true ranges and offsets due to user time error.

Position determination by use of GPS involves the use of spread-spectrum techniques for separating the signals from a particular satellite from those of other satellites in the field of view and for obtaining precise range values. The signals are received at low levels, usually well below the thermal noise level in the receiver. Each satellite operates with a unique P code, XP_i, which is generated from the product of two PN (pseudonoise) codes, Xl (t) and X2 ($t + n_i T$), where T is the 10.23 MHz clock period and n_i takes on values from O to 36 (Spilker, 1980). Code Xl has a period of about 1.5 s or 15,345,00 chips and code X2 is 37 chips longer.

If an XP code is allowed to continue without resetting it would have a period without repetition of about 267 days but the code of each satellite is reset to its initial condition every seven days, allowing each satellite a unique seven-day segment of the long code, Thus it can be considered that there is really only one long code and that the different satellites use different parts of it.

Each satellite also transmits a shorter C/A code, XG(t), of 1023 bits or about 1 ms, based on a repetition rate of 1.023 MHz, This code is used for signal acquisition. The C/A code is a Gold code formed as the product of two 1023 bit PN codes, G 1 (t) and G2[t + N_1 (1OT)] where T is the period of 10.23 MHz and N_i can take on any of 1023 values. The total signal SL 1 (t) transmitted on the L1 frequency (1575.42 MHz) is given by

$$SL1_i(t) = A_p XP_i(t)D_i(t)\,et).s(ult + \phi) + A_c XG_i(t)D_i(t)\sin(\omega_1 t + \phi) \quad (6.61)$$

The A's are amplitudes, XP_I is the P code, XG_I is the C/A code, and D_1 (t) carries data at 50 bps on satellite status, satellite position (ephemeris data), errors of the satellite cesium clock, and parameters for correcting for ionospheric excess time delay. The data channel has a 30 s overall frame period and 6 s subframes. The signal SL2 (t) at 1227.60 MHz may be modulated by a P code or a C/A code. Assuming modulation bya Pcode, it has the form of

$$SL2_i(t) = B_p XP_i(t)D_i(t)\cos(\omega_2 t + \theta) \quad (6.62)$$

where B_p is amplitude.

Using the 1023 chip XG_i (t), it takes about 45 s or more to establish synchronism of the transmitter and receiver codes. Search must be carried out in both time and frequency as signals from the satellites are Doppler shifted in frequency. The overall time uncertainty is 1023 μs and the frequency uncertainty may be in the order of 10 kHz, compared to an IF bandwidth of 1 kHz. Once the transmitted C/A code has been acquired, the 50 bps data carried by D_i (t) is received. A new HOW word (Hand-Over-Word) that is transmitted every 6 s in the data stream then indicates the correct

phase point in the incoming P code, and the user equipment is shifted in phase to synchronize with the incoming P code at the next change in the HOW.

From the propagation viewpoint, ionospheric and tropospheric excess range delay and multipath effects are of practical importance. For the frequencies utilized, ionospheric excess range delay AR at the frequency L 1 is related to differential range delay δR between the two frequencies by

$$AR = 1.5336\ \delta R \tag{6.63}$$

The concept of correcting for ionospheric excess range delay by use of two frequencies was presented in Sec. 2.3.1. The ionosphere also modifies Doppler frequency by an amount Δf_{L1} given by

$$\Delta f_{L1} = 3.529\ \delta f \tag{6.64}$$

for the frequencies utilized, where δf is the differential Doppler frequency between the two frequencies. The 18 GPS satellites will be in six oribital pines inclined at 55 de with respect to the equator and spaced 60 deg in longitude, with?t-ee satellites in each oribital plane. The true difference in radial velocity of two satellites, one approaching and one receding from a stationary observer at the north pole where there is zero effect from rotation of the Earth, generates a Doppler frequency difference of 7500 Hz (Spilker, 1980).

Excess range delay due to dry air can be determined and corrected for with high accuracy (Sec. 3.7). The delay due to water vapor is more difficult to determine precisely. Its small magnitude may not be important for routine applications but will be important when high precision is desired, as for geodetic applications. To obtain the highest precision use canbe made of carrier phase. This approach requires measures to resolve the inherent ambiguity of multiples of 2π radians in phase (Counselman and Gourevitch, 198 1; Brown and Hwang, 1 983). One reference reports position errors of 1.2 to 2.7 m due to multipath effects, using standard techniques rather than carrier phase (Milliken and Zoner, 1978). The wide bandwidth of GPS provides frequency diversity and the effect of multipath would be expected to be greater for narrowband operationat the same nominal frequency.

The quantity PDOP (Position Dilution of Precision) represents the ratio of $Ap = [(Ax)^2 + (\Delta y)^2 + (Az)^*]^{1/2}$ to Δr where Ap is rms position error, expressed in terms of errors in x, y, and z coordinates, and Ar is rms radial range error (Spilker, 1980). It develops that PDOP is likely to have a value of about three or less. If position is to be determined to an accuracy of 10 m, then radial range must be measured to an accuracy of 10/3, Determining the distance between the user's position and that of a satellite involves shifting the phase of the receiver code until maximum correlation is obtained with the incoming signal (Parkinson and Gilbert, 1983). If the phase were to be shifted continuously over a range including that of the maximum signal amplitude, GPS could apparently be used to obtain multipath data (Sec. 6.3.1).

Important impending applications of GPS are to determining satellite orbits and geodetic baselines. The Ocean Topographic Experiment (TOPEX) satellite, scheduled for launch in the early 1990's, will have a GPS receiver on board, and signals from four GPS satellites will be used to determine the position of the satellite (Yunck, Wu, and Lichten, 1985). A differential GPS technique that will be employed will actually involve determining the satellite position with respect to ground receivers at precisely known locations. As suggested by Fig. 6.26, pseudo ranges to two receivers, one on the ground and one in the TOPEX satellite, will be measured. From such a measurement utilizing one GPS satellite, the projection of the distance B between the ground receiver and satellite in the direction of ρ_u of Fig. 6.26 is found. By using four satellites, the magnitude and direction of B is completely determined and the satellite position is thus also known, The differential technique has the advantage of tending to eliminate clock error and errors in positions of the GPS satellites, as their errors are common to both transmission paths along ρ_u and ρ_s of Fig. 6.26. The use of carrier phase will allow determining position rapidly and precisely , and the combination of pseudo range and phase measurements is expected to give better results than either alone, Because the satellite frequencies are not widely separated, it is expected that the use of Eq. (6.54) will not correct for ionospheric delay as precisely as desired, but long-term averaging, the hybrid strategy of using both pseudo range and carrier phase, and

simultaneous solutions for both the TOPEX and GPS orbits should allow decreasing the ionospheric as well as other errors to a high degree. Attention is also being given to GPS receiver design, antemas that discriminate against multipath, and the use of water-vapor radiometers to determine the excess range delay due to water vapor.

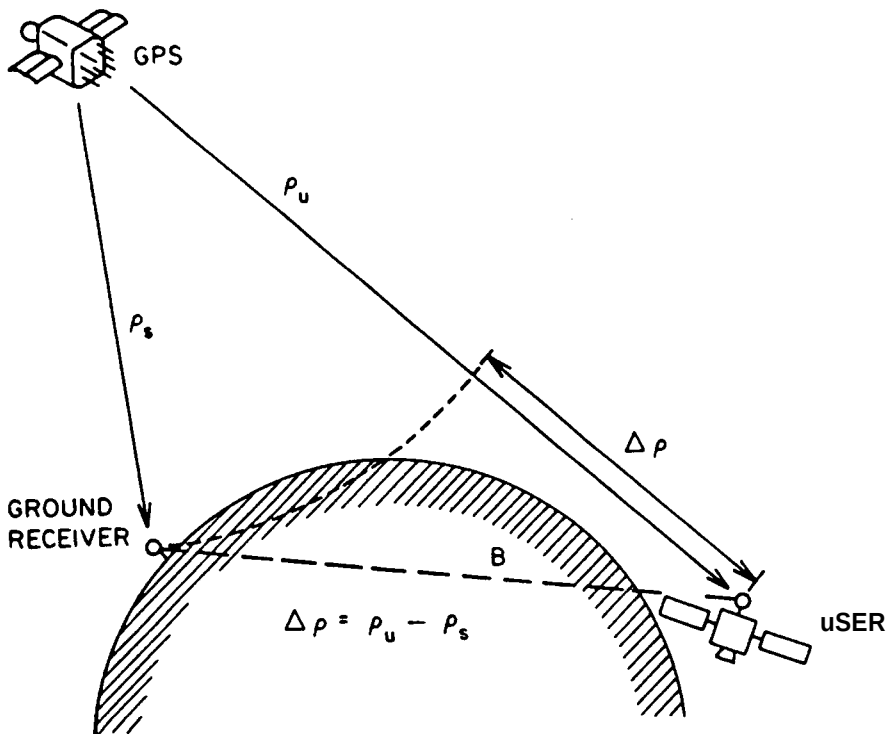

Figure 6.26. Differential technique for utilizing GPS.

REFERENCES

Assis, M. S., "A simplified solution to the problem of multiple diffraction over rounded obstacles," IEEE Trans. Antennas Propagat., vol. AP-19, pp.292-295, March 1971.

Barnwell, T. P. , " Development, design, fabrication, and evaluation of a broadband speech compression system at 4800 bits per second, " Session 2, Mobile Satellite Industry Briefing, (viewgraphs) Jet Propulsion Lab., Nov. 13-14, 1985.

Barrow, B. B., L. G. Abraham, W. M. Cowan, and R. M. Gallant, "Indirect atmospheric measurements utilizing. rake tropospheric scatter techniques - Part I: The rake tropospheric scatter technique." Proc. IEEE, vol. 57, pp. 537-551, April 1969.

Bateman, A. J., G. Lightfoot, A. Lymer, and J. P. McGeehan, "Speech and data communications over 942 MHZ TAB and TTIB single sideband mobile radio systems incorporating feed-forward signal regeneration, " IEEE Trans. Veh. Technol., VT-34, pp.13-21, Feb. 1985.

Beckmann, P., Probability in Communication Engineering. New York: Harcourt, Brace & World, 1967.

Beckmam, P. and A. Spizzichino, The Scattering of Electromagnetic Waves from Rough Surfaces. New York: Macmillan Co. 1963.

Bitzer, D R., et al., "A rake system for tropospheric scatter," IEEE 'Trans. Comm., vol. COM-14, pp.496-506, Aug. 1966.

Book, S. A., W. F. Brady, and P. K. Mazaika, "The nonuniform GPS constellation," in IEEE 1980 Position Location and Nav. Sym. Record, pp. 1-8. New York: Inst. of Elect. and Electronic Eng., 1980.

Boudreau, P. M. and A. L. Barry, "The Canadian MSAT program," in Satellite Systems for Mobile Communications and Navigation, pp. 28-32. London & New York: IEE, 1983

Brisken, A. F., R. E. Anderson, R. L. Frey, and "J, R. Lewis, "Land mobile communications and position fixing using satellites," IEEE Trans. Veh. Technol., vol. VT-28, pp. 153-170, Aug. 1979.

Brown, R. G. and P. Y. C. Wang, "A Kalman filter approach to precision GPS geodesy," Navigation vol. 30, pp. 338-349, Winter, 1983-1984.

Bullington, K., "Radio propagation for vehicular communications," IEEE Trans. Veh. Technol., vol. VT-26, pp. 295-308, Nov. 1977.

Butterworth, J. S. and E. E. Mott, "The characterization of propagation effects for land mobile satellite services," in Satellite Systems for Mobile Communications and Navigation, London and New York: IEE. 1983.

Butterworth, J. S., "Propagation data for land mobile satellite system,", pp. 371-378, Pmt. of NAPEX VIII, Jet Propulsion Lab., Pasadena, CA, June 20-21, 1985.

CCIR, "Multipath effects in aircraft-to-satellite communication and radio determination links," Report 505-2 in Vol. VIII, Mobile Services, Recommendations and Reports of the CCIR 1978. Geneva: Int. Telecomm. Union, 1978.

CCIR, "Propagation data for maritime and land mobile satellite systems above 100 MHz," Report 884 in Vol. V, Propagation in Non-ionized Media, Recommendations and Reports of the CCIR. 1982. Geneva: Int. Telecomm. Union, 198 .

CCIR, Proposed Modifications to Report 884, Propagation Data for Maritime Mobile Satellite Systems for Frequencies Above 100 MHz, CCIR Study Group Dec. 5/102-E, 2 Aug. 1983.

CCIR, "Ground-wave propagation curves for frequencies between 10 kHz and 30 MHz," Recommendation 368-5 in Vol. V, Propagation in Non-ionized Media, Recommendations and Reports of the CCIR, 1986. Geneva: Int. Telecomm. Union, 1986a.

CCIR, "Propagation by diffraction," Report 715-2 in Vol. V, Propagation in Non-ionized Media, Recommendations and Reports of the CCIR, 1986. Geneva: Int. Telecomm. Union, 1986b.

CCIR. "Reflection from the surface of the Earth," Report 1008 in Vol. V, Propagation in Non-ionized Media, Recommendations and Reports of the CCIR, 1986. Geneva: Int. Telecomm. Union, 1986c.

CCIR. "Electrical characteristics of the surface of the Earth," Recommendation 527-1 in Vol. V, Propagation in Non-ionized Media, Recommendations and Reports of the CCIR, 1986. Geneva: Int. Telecomm. Union, 1986d.

CCIR, "Propagation data for maritime mobile-satellite systems for frequencies above 100 MHz," Report 884-1 in Vol. V, Propagation in Non-ionized Media, Recommendations and Reports of the CCIR, 1986. Geneva: Int. Telecomm. Union, 1986e.

CCIR, "Propagation data for land mobile-satellite systems for frequencies above 100 MHz," Report 1009 in Vol. V, Propagation in Non-ionized Media, Recommendations and Reports of the CCIR, 1986. Geneva: Int. Telecomm. Union, 1986f.

CCIR, "Maritime satellite system performance at low elevation angles." Report 920-1 in Vol. VIII-3, Mobile Services, Recommendations and Reports of the CCIR, 1986. Geneva: Int. Telecomm Union., 1986g.

CCIR, "Link power budgets for a maritime mobile satellite service," Repor 760-1 in ol. VIII, Mobile Services, Recommendations and Reports of the CCIR, i 986. Geneva: Int. Telecomm. Union., 1986h.

CCIR, "Ionospheric effects upon earth-space propagation," Report 263-6 in Vol. VI, Propagation in Ionized Media, Recommendations and Reports of the CCIR, 1986. Geneva: Int. Telecomm. Union. 1986i.

CCIR, "Man-made radio noise," Report 258-4 in Vol. VI, Propagation in Ionized Media, Recommendations and Reports of the CCIR, 1986. Geneva: Int. Telecomm. Union, 1986j.

Cooper, G. R. and R. W. Nettleton, "A spread-spectrum technique for high-capacity mobile communications," IEEE Veh. Technol., vol. VT-27, pp. 264-275, Nov. 1978.

Cooper, G. R. and R. W. Nettleton, "Cellular mobile technology: the great multiplier," IEEE Spectrum, vol. 20, pp. 30-37, June 1983.

Counselman, C. C. and S. A. Gourevitch, "Miniature interferometer terminals for earth surveying: ambiguity and multipath with Global Positioning System," IEEE Trans. Geosci. Rem. Sens., vol. GE-19, pp. 244-252, Oct. 1981.

Cox, D. C., "910 MHz urban mobile radio propagation: multipath characteristics in New York City," IEEE Trans. Comm,, vol. COM-21, pp. 1188-1194, Nov. 1973.

da Silva Curiel, A., "The first generation INMARSAT system," in Satellite Systems for Mobile Communication and Navigation, pp. 1-7. London & New York: IEE, 1983.

/avarian, F., "Fade margin calculation for channels impaired by Rician fading," IEEE Trans. Veh. Technol. vol. VT-34, pp. 41-44, Feb. 1985.

Davarian, F., "Channel simulation to facilitate mobile-satellite communications research," IEEE Trans. Comm., vol COM-35, pp. 47-56, Jan. 1987.

Deygout, J., "Multiple knife-edge diffraction of microwaves," IEEE Trans. Veh., Technol. Vol. 480-489, July, 1 966.

Divsalar, D. "Trellis coded modulation for 4800 bps and 9600 bps in 5 kHz channels," Session 2, Mobile Satellite Industry Briefing (viewgraphs), Jet Propulsion Lab., Nov. 13-14, 1985.

Dixon, R. C., Spread Spectrum Systems, New York: Wiley, 1976.

Espeland, R. H., E. J. Violette, and K. C. Allen, Atmospheric Channel Performance Measurements at 10 to 100 GHz, NTIA Report 84-149, U. S. Department of Commerce, April 1984.

Fang, D. J., T. S. Tseng, and T. O. Calvit, "A low elevation angle propagation measurement of i .5-GHz satellite signals in the Gulf of Mexico," IEEE Trans. Ant. Propagat., vol. AP-30, pp. 10-15, Jan. 1982.

Fang, D.J. and R.H. Ott, "A low elevation angle L-band maritime propagation measurement," in Satellite Systems for Mobile Communications and Navigation, pp. 45-50. London and New York: IEE. 1983.

Flock, W. L., Electromagnetic and the Environment: Remote Sensing and Telecommunications. Englewood Cliffs, NJ: Prentice-Hall, 1979.

General Electric, "Pilot tone calibration techniques," Session 2, Mobile Satellite Industry Briefing (v iewgraphs), Jet Propulsion Lab., Pasadena, CA, Nov. 13-14, 1985.

Gersho, A., "Development, design, fabrication, and evaluation of a broadband speech compression systems at 4800 bits per second," Session 2, Mobile Satellite Industry Briefing (viewgraphs), Jet Propulsion Lab., Nov. 13-14, 1985.

Goldhirsh, J. and W. J. Vogel, "Roadside tree attenuation measurements at UHF for land mobile-satellite systems," IEEE Trans. Antennas Propagat., vol. AP-35, pp. 589-596, May 1987.

Hall, M.P.M., Effects of the Troposphere on Radio Communication. Stevenage, U. K. and New York: Peter Peregrinus for IEE, 1979.

Hansen, F. and F. I. Meno, "Mobile fading - Rayleigh and lognormal superimposed," IEEE Trans. Veh. Technol., vol. VT-26, pp. 332-335, Nov. 1977.

Hess, G. C., "Land-mobile satellite excess path loss measurements," IEEE Trans. Veh. Technol., vol. VT-29, pp. 290-297, May 1980.

Hufford, G. A. et al. Wideband Propagation Measurements in the Presence of Forests, OFCOM 82-CS029-F, U. S. Army Communications-Electronics Command, Fort Monmouth NJ 07703, Jan. 1983.

Jakes, W. C., Microwave Mobile Communications. New York: Wiley, 1974.

Jenkins, F. A. and H. E. White. Fundamentals of Optics, 4th ed. New York: McGraw-Hill, 1976.

Jordan, E. C. and K. C. Balmain, Electromagnetic Waves and Radiating Systems. Englewood Cliffs, NJ: Prentice-Hall, 1968.

Kirby, R. S., H. T. Dougherty, and P. L. McQuate, "Obstacle gain measurements over Pikes Peak at 60 to 1,046 Mc," Proc. IRE, vol. 43, pp. 1467-1472, Oct. 1955.

Knouse, G. H., "Terrestrial land mobile satellite considerations, NASA plans and critical issues," IEEE Trans. Veh. Technol. vol. VT-29, pp.370-374, Nov. 1980.

Lipke, D. W. et al., "MARISAT - a maritime satellite communication system," COMSAT Technical Rev., vol. 7, pp.351-392, Fall 1977.

Loo, C., "A statistical model for a land mobile satellite link," IEEE Trans. Veh. Technol. vol. VT-34, pp. 122-127, Aug. 1985.

Miller, A. R., R. W. Brown, and E. Vegh, "New derivation for the rough-surface reflection coefficient and for the distribution of sea-wave elevations," IEE Proc., vol. 131, Part H, pp. 114-116, April 1984.

Milliken, R. J. and C. J. Zoner, "Principle of operation of NAVSTAR and system characteristics," Navigation, vol. 25, pp. 95-106, Summer 1978.

Norton, K. A., P. L. Rice, and L. E. Vogler, "The use of angular distance in estimating transmission loss and fading rate for propagation through a turbulent atmosphere over irregular terrain," Proc. IRE, vol. 43, pp. 1488-1526, Oct. 1955.

Ott, R. H., "An alternative integral equation for propagation over irregular terrain," Radio Sci., vol. 6, pp. 429-435, 1971.

Parkinson, B. W. and S. W. Gilbert, "NAVSTAR: Global Positioning System - ten year's later," Proc. IEEE, vol. 71, pp. 1177-1186, Oct. 1983.

Panter, P. F,, Communication Systems Design. New York: McGraw-Hill. 1972.

Price, R. and P. E. Green, "A communication technique for multipath channels," Proc. IRE, vol. 46, pp. 555-570, March 1958.

Proakis, J. G., Digital Communications. New York: McGraw-Hill, 1983.

Qureshi, S. "Adaptive equalization," IEEE Commun. Msg., vol. 20, pp. 9-16, March 1982.

Sass, P. F., "Propagation measurements for UHF spread spectrum mobile communications," IEEE Trans. Veh. Technol., vol. VT-32, pp. 168-176, May 1983.

Schwartz, M,, W. R. Bennett, and S. Stein, Communication Systems and Techniques. New 1966.

Simon, M. K. "Digital modulation for narrow-band fading satellite channels," Session 2, Mobile Satellite Industry Briefing (viewgraphs), Jet Propulsion Lab., Pasadena, CA, Nov. 23-14, 1985.

Sheperd, N. M., "Radio wave loss deviation and shadow loss at 900 MHz," IEEE Trans. Veh. Technol., vol. VT-26, pp. 309-313, Nov. 1977.

Smith, E. K., "Multipath, trees, scintillation, and noise," unpublished presentation at NAPEX IX, U. of Colorado, Boulder, CO, Jan. 16, 1986.

Spilker, J. J., "GPS signal structure and performance characteristics," Navigation, vol 25, pp. 121-146, Summer 1978. (Also pp. 29-54 in Global Positioning System, Papers published in Navigation, vol. 1, 1980).

Stutzman, W. , "PELMOSS modeling," pp 343-363 in JPL D-2619, Proc. of NAPEX VIII, June 20, 1985 at U. of British Columbia; Jet Propulsion Lab., Pasadem, CA, Ag. .26, 1985.

Sue, M.K. (cd.), An Aeronautical Mobile Satellite System, Part I, Executive Summary; Part II, Technical Report. Pasadena: Jet Propulsion Laboratory, September 1, 1987.

Townes, S. A., "Near toll quality digital speech at 4800 bps," Session 2, Mobile Satellite Industry Briefing (viewgraphs), Jet Propulsion Lab., Pasadena, CA, Nov. 13-14, 1985.

Turin, G. L., "Introduction to spread-spectrum antimultipath techniques and their application to urban digital radio," Proc. IEEE, vol. 68, pp. 328-353, March 1980.

Vogel, W. J., Land mobile radio propagation measurements at 869 and 1501 MHz," pp. 261-281 in JPL D-2619, Proc. of NAPEX VIII, June 20, 1985 at U. of British Columbia; Jet Propulsion Lab., Pasadena, CA, Aug. 26, 1985.

Vogel, W. J. and G. W. Torrence, Measurements Results from a Balloon Experiment Simulating Land Mobile Satellite Transmissions," Elect. Eng. Research Lab., U. of Texas Austin, TX 78758, 30 April 1984.

Vogel, W. J. and E. K. Smith, Propagation Considerations in Land Mobile Satellite Transmission, MSAT-X Report No. 105, Jet Propulsion Lab., Pasadena, CA, 24 Jan. 1985.

Vogel, W. J. and J. Goldhirsh, "Tree attenuation at 869 MHz derived from remotely piloted aircraft measurements," IEEE Trans. Antennas Propagat., vol. AP-34, pp. 1460-1464, Dec. 1986.

Vogel, W. J. and J. Goldhirsh, "Fade measurements at L-band and UHF in mountainous terrain for land mobile satellite systems," IEEE Trans. Antennas Propagat., vol. AP-36, Jan. 1988.

Weber, W. J. and F. Naderi, "NASA mobile satellite experiment (MSAT-X)," in Pmt. Nat. Electronics Conf., Chicago, IL, 1983, vol. 37, pp. 328-330, 1983.

Yeh, Y. S. and D. O. Reudink, "Efficient spectrum utilization for mobile radio systems using space diversity," IEEE Trans. Comm., vol. COM-30, pp. 447-455, March 1982.

Yunck, T. P., S-C. Wu, and S. M. Lichten, "A GPS measurement system for precise satellite tracking and geodesy," J. Astronautical Sciences, VOL 33, pp. 367-380, Oct.-Dec. 1985.

APPENDIX 6.1

REFLECTION COEFFICIENTS FOR CIRCULAR POLARIZATION

An electric field intensity vector E of arbitrary polarization can be expressed in terms of either circular or rectangular components as indicated by

$$\mathbf{E} = {}'R\ a_r + {}'L\ \mathbf{a}_l = E_x \mathbf{a}_x + E_y \mathbf{a}_y \qquad \text{(A6.1)}$$

where E_R, EL, E_x, and E_y are in general complex quantities. The a's represent unit vectors, with a_r a vector of unit length that is rotating in the right circular direction with angular ω where ω is the angular wave frequency, The unit vector $\mathbf{a}_l$ represents a unit vector rotating in the left circular direction, and $\mathbf{ax}$ and $\mathbf{a}_y$ are unit vectors in the x and y directions. The unit vectors $\mathbf{a}_r$ and $\mathbf{a}_l$ can be expressed in terms of ax and $\mathbf{a}_y$ by

$$\mathbf{a}_r = \mathbf{a}_x - \text{jay}, \qquad \mathbf{a}_l = \mathbf{a}_x + j\mathbf{a}_y \qquad \text{(A6.2)}$$

If these definitions of $\mathbf{a}_r$ and $\mathbf{a}_l$ are substituted into Eq. (A6. 1), it develops that

$$ER+EL=E_x \qquad \text{(A6.3)}$$

and

$$'R - 'L = jE_y \qquad \text{(A6.4)}$$

These two equations can be treated as two equations for two unknowns, E_R' and EL. Solving for these quantities by use of determinants or otherwise,

$$E_R = \frac{E_x + jE_y}{2} \qquad \text{(A6.5)}$$

and

$$E_L = \frac{E_x - jE_y}{2} \qquad \text{(A6.6)}$$

The field components E_x and E_y are total field components, and the relations apply to any combination of right and left circularly

polarized waves and also when only right or left circular waves are present. For example, consider that only a right circular wave is present. For this case, $E_y = -jE_x$,

$$E_R = \frac{E_x + j(-jE_x)}{2} = E_x, \qquad \text{(A6.7)}$$

and

$$E_L = \frac{E_x - j(-jE_x)}{2} = 0 \qquad \text{(A6.8)}$$

Consider further that a right circular wave is incident upon a flat, smooth surface. Using the subscript i to refer to the incident wave, it can be determined from Eq. (A6.7) that $E_{Ri} = E_{xi}$. Next consider the wave resulting from reflection of this incident right circular wave. Taking E_x to refer to the horizontal component of the reflected wave, E_x is given by

$$E_x = \rho_h E_{xi} = \rho_h E_{Ri} \qquad \text{(A6.9)}$$

where ρ_h is the reflection coefficient for horizontal polarization. Likewise for E_y, the vertical component of the reflected wave,

$$E_y = \rho_v E_{yi} = \rho_v(-jE_{xi}) = -j\rho_v E_{Ri} \qquad \text{(A6.10)}$$

Thus for the reflected wave, using Eq. (A6.5),

$$E_R = \frac{\rho_h E_{Ri} + j(-j\rho_v E_{Ri})}{2}$$

and

$$E_R = \frac{\rho_h E_{Ri} + \rho_v E_{Ri}}{2} \qquad \text{(A6.11)}$$

Finally divide both sides of Eq. (A6. 11) by E_{Ri} and identify ER/ERi as ρ_c, the reflection coefficient for the copolarized component of the reflected wave, The result is that

$$\rho_c = E_R/E_{Ri} = \frac{\rho_h + \rho_v}{2} \qquad \text{(A6.12)}$$

The same substitutions can be made in Eq. (A6. 6) and one can divide by E_{Ri} again but now E_L/E_{Ri} represents ρ_x, the reflection coefficient giving the crosspolarized component of the reflected wave. Following this approach

$$'L = \frac{\rho_h E_{Ri} - j(-j\rho_v E_{Ri})}{2} = \frac{\rho_h E_{Ri} - \rho_v E_{Ri}}{2}$$

and

$$\rho_x = E_L/E_{Ri} = \frac{\rho_h - \rho_v}{2} \qquad \text{(A6.13)}$$

If consideration is given to an incident left circularly polarized wave, and the type of pocedure utilized above is employed again but it is recognized that $E_{yi} = jE_{xi}$ and $E_y = j\rho_v R_{Li}$ for left circular polarization, the same relations, namely Eqs. (A6. 12) and (A6. 13), are obtained.

The basic relations of Eqs. (A6. 1) through (A6.6) aregiven in a number of references, for example Weeks (1964). A combination of right and left circularly polarized waves constitutes an elliptically polarized wave having an axial ratio (A. R.) given by

$$A.R. = \frac{|E_R| + |E_L|}{|E_R| - |E_L|} \qquad \text{(A6.14)}$$

This ratio represents the ratio of the major axis of. the polarization ellipse to the minor axis. The angle of the major axis of the ellipse, with respect to a reference axis, is halfway between instantaneous positions of the right and left circular components, consistent with Eq. (2.23) for Faraday rotation.